



Forschungszentrum Karlsruhe
Technik und Umwelt

Wissenschaftliche Berichte
FZKA 6074

Monte Carlo Analysis of the Low-Temperature Adsorption Facility TITAN and its Pumping Characteristics

A. Schwenk-Ferrero, Chr. Day

**Hauptabteilung Ingenieurtechnik
Projekt Kernfusion**

März 1998

Forschungszentrum Karlsruhe

Technik und Umwelt

Wissenschaftliche Berichte

FZKA 6074

**Monte Carlo Analysis of the Low-Temperature Adsorption
Facility TITAN and its Pumping Characteristics**

A. Schwenk-Ferrero, Chr. Day

Hauptabteilung Ingenieurtechnik
Projekt Kernfusion

Forschungszentrum Karlsruhe GmbH, Karlsruhe
1998

Als Manuskript gedruckt
Für diesen Bericht behalten wir uns alle Rechte vor
Forschungszentrum Karlsruhe GmbH
Postfach 3640, 76021 Karlsruhe
Mitglied der Hermann von Helmholtz-Gemeinschaft
Deutscher Forschungszentren (HGF)
ISSN 0947-8620

Abstract

Within the framework of the European Fusion Technology Programme, the Karlsruhe Research Centre (FZK) has been charged with the development of the primary vacuum pumping system for the International Thermonuclear Experimental Reactor ITER. To support the design and operation of the cryopump, an experimental campaign for pump component testing was started at the TITAN test facility available in FZK. The primary objective was to investigate, under ITER-relevant conditions, the pumping speed of the designed cryosorption panels coated with activated carbon. The experiments performed at TITAN allow to determine the relationship between the pumping speed of the gas, the gas load and the pressure during pumping. The pumping speed strongly depends on the arrival rate of the gas, the geometry of the pumping system, the cold surface, the type of sorbent used, the temperature and the gas load.

In order to quantify the geometry impact on the measured pumping speed in the molecular flow regime, the Monte Carlo method was applied. To analyse the rarefied gas flow in the TITAN test facility, the general Monte Carlo code MOVAK3D was employed. A series of simulations was performed to determine the conductance of the entire TITAN vacuum structure, to evaluate the capture probability depending on the panel pumping characteristics, to gain an insight into the relative pressure variation within the structure and finally to study the influence of panel arrangement on the TITAN overall pumping performance.

As a result of this analysis, the two most important integral characteristics of the TITAN pumping system the transmission probability and the capture probability could be evaluated. It could be demonstrated that the conductance of the TITAN structure components (the integral transmission probability amounts to 0.1) causes a significant decrease of the measured pumping speed as compared to the potential pumping speed of the panel. The capture probability was shown to be strongly dependent on the gas sticking coefficient of the charcoal sorbent material. The maximum value attainable for the sticking coefficient equalling unity was estimated to be 0.0915 for the structure with the quilted panel and 0.085 for the structure with the circular panel. The simulations confirmed that the pressure in the pump is reduced by approximately one order of magnitude, relative to the pressure in the vacuum chamber. Additionally, for the panel in quilted geometry, the contribution to the overall capture probability by the rear and front panel side was quantitatively estimated for different panel incline to the gas entry plane.

Moreover, an analytical formula describing the dependence of the capture probability on both the sticking coefficient and the transmission probability was derived for the TITAN geometrical configuration. A method to determine the sticking coefficients from the measured quantities was proposed and successfully applied. The results for pure helium were compared with those for helium/hydrogen mixtures to illustrate and discuss potential difficulties of pump operation.

Monte Carlo Analyse für die Tieftemperaturanlage TITAN und deren Pumpcharakteristiken

Kurzfassung

Im Rahmen des 'European Fusion Technology Programme' werden bei FZK Entwicklungsarbeiten für das primäre Vakuumpumpsystem des Fusionsreaktors ITER durchgeführt. Für die Auslegung und den Betrieb der Kryopumpe wurden in einer unterstützenden Versuchsreihe Komponenten an der Anlage TITAN getestet. Das primäre Ziel dabei war es, das Saugvermögen der mit Aktivkohle beschichteten Kryosorptionspanels unter ITER-relevanten Bedingungen zu ermitteln. Die TITAN-Experimente erlauben die Bestimmung des Zusammenhangs von Saugvermögen, Gasbeladung und Druck während des Pumpens. Das Saugvermögen hängt dabei vom Durchsatz des zu prozessierenden Gases ab, von der Geometrie des Pumpsystems, von der kalten Pumpfläche, vom Typ des Sorbentmaterials, von der Temperatur und von der Gasbeladung.

Um den Einfluß der Geometrie auf das gemessene Saugvermögen im molekularen Strömungsbereich quantitativ zu ermitteln, wurde die Monte Carlo Methode verwendet. Die verdünnte Gasströmung in der TITAN-Anlage wurde mit dem Monte Carlo Code MOVAK3D modelliert. In einer Reihe von Simulationsrechnungen sollte der Leitwert der wesentlichen Vakuumbaulemente von TITAN und die Abhängigkeit der Einfangwahrscheinlichkeit vom Betriebszustand des Panels bestimmt werden. Darüber hinaus sollten die relativen Druckunterschiede innerhalb der Anlage und der Einfluß der Panelanordnung auf das Pumpverhalten untersucht werden.

Als Hauptergebnis der Monte Carlo Analyse wurden die beiden wesentlichen Betriebscharakteristiken der TITAN-Anlage, nämlich die Durchtrittswahrscheinlichkeit und die Einfangwahrscheinlichkeit ermittelt. Dabei zeigte sich, daß der niedrige integrale Leitwert der TITAN-Einbauten (Durchtrittswahrscheinlichkeit von 0.1) das gemessene Saugvermögen im Vergleich zu dem Saugvermögen direkt am Kryopanel deutlich herabsetzt. Die Einfangwahrscheinlichkeit hängt stark vom Sticking-Koeffizient (der Haftwahrscheinlichkeit) am Aktivkohlematerial ab. Der maximale Wert, der bei einem Sticking-Koeffizienten von Eins erreicht wurde, beträgt 0.0915 für die Geometrie mit einem Rechteckpanel in 'Quilted design' und 0.085 bei der Verwendung eines kreisrunden Panels. Ferner zeigten die Simulationsrechnungen, daß der Druck über der pumpenden Fläche ungefähr eine Größenordnung kleiner ist als in der Meßebeine. Außerdem wurde für den Fall des Rechteckpanels quantitativ berechnet, wie sich die gesamte Einfangwahrscheinlichkeit des Panels für verschiedene Anstellwinkel relativ zur Strömungsrichtung auf die verschiedenen Panelseiten verteilt.

Darüber hinaus wurde für die TITAN Geometrie ein geschlossener Ausdruck hergeleitet, der es ermöglicht, die Abhängigkeit der Einfangwahrscheinlichkeit vom Sticking-Koeffizienten und der Durchtrittswahrscheinlichkeit zu ermitteln. Eine Methode zur Ableitung von Sticking-Koeffizienten aus den Meßgrößen wurde

entwickelt und erfolgreich angewendet. Die Ergebnisse für reines Helium und Helium/Wasserstoff-Mischungen wurden verglichen, um mögliche kritische Betriebszustände herauszufinden.

Contents

1	Introduction	1
2	Estimation of integral characteristics of a vacuum system by the Monte Carlo method	4
3	An overview of the Monte Carlo Code MOVAK3D and its main features	5
4	Geometrical model of the TITAN structure for the analysis with MOVAK3D.....	7
5	Specification of the computational task.....	13
6	Presentation and discussion of the Monte Carlo simulation results.....	18
6.1	Pumping system characteristics	18
6.1.1	Transmission probability.....	18
6.1.2	Capture probability	19
6.2	Conductance.....	20
6.3	Net pumping speed.....	21
6.4	Relative pressure.....	23
6.5	Capture probability depending on panel incline	26
6.6	Panel pumping performance.....	28
7	Evaluation of sticking coefficients	28
7.1	Investigation for pure helium gas	31
7.2	Investigation for helium-containing mixtures.....	33
8	Application limits of the test-particle Monte Carlo method.....	36
9	Remarks on the Monte Carlo precision.....	37
10	Conclusions	39

1 Introduction

Within the framework of the development of the primary vacuum pumping system for ITER, a conceptual study for the prototype cryopump was accomplished and the model cryopump has already been designed. Its suitability to fulfill the ITER relevant conditions will be investigated experimentally in the near future. Prior to the construction of the prototype cryopump, an extensive testing programme had to be carried out in order to assess the pumping performances of the pump test components. For this purpose, a versatile test facility, TITAN (Tief-Temperatur-Adsorption), was set up at the Central Engineering Department of the Karlsruhe Research Centre (FZK).

The TITAN experimental facility represents a shielded cryopump installed in the test vessel. A cylindrical vacuum vessel of 700 mm diameter and 2200 mm height (free volume 0.76 m³) is designed as a measuring dome in compliance with the PNEUROP standard for vacuum pump testing [1]. To fulfill the requirements of the "constant pressure method" for deriving the pumping speed from the measured throughput and pressure, the gas is admitted centrally and vertically downwards into the lower part of the vessel from a tube of 70.3 mm inner diameter bent through a right angle. The cryopump consists of a cryopanel which is covered on one or both sides with an activated charcoal (Chemviron SCII) sorbent material, fixed to the metallic substrate of the panel by an inorganic cement (Thermoguss 2000). To minimise heat loads on the panel, caused by thermal radiation through the pump inlet, a LN₂ pool-cooled 106° chevron baffle, copper-made and blackened, was installed. The panel and the baffle are accommodated in the pump housing. The shield maintained at 80K is incorporated on the inside. The baffle is screwed to the bottom of a cylindrical annular LN₂ recipient and kept at 80K by heat conduction. The panel is placed in the centre of the 80K volume which is covered from the top by a copper plate.

In order to assess the pumping performance of a recommended cryopanel design under the ITER-relevant conditions, an extensive experimental testing programme was performed at the TITAN facility during the last five years. Its principal goal was to determine the pumping speed of the selected cryopanel which should be able to pump down the plasma exhaust gas components, such as the hydrogen isotopes (protium, deuterium and tritium), helium and impurities. The key scaling parameter involved in the transfer from component test results to the ITER pump is the specific, i.e. related to the panel surface, pumping speed of about 1 l/(s·cm²) at a maximum

specific gas load of about $0.23 \text{ (Pa}\cdot\text{m}^3\text{)/cm}^2$, corresponding to 900 s pumping time, except for pure helium, where the operation times are limited [2].

In the TITAN facility two different cryosurfaces were investigated:

- the circular adsorption panel (1186 cm^2 pumping surface), bolted to the bottom of the centrally placed LHe bath container, arranged orthogonally to the gas flow direction,
- the rectangular adsorption panel (3500 cm^2 pumping surface) in quilted design geometry ($0.35 \text{ m} \times 0.5 \text{ m}$, channel pitch 50 mm), which is foreseen for the ITER primary cryopump, installed in parallel to the gas flow direction.

Dosage rates of the gas can be varied from $2.5\cdot 10^{-3} \text{ (Pa}\cdot\text{m}^3\text{)/s}$ to $1.69 \text{ (Pa}\cdot\text{m}^3\text{)/s}$ (at 273,15K) employing three mass flow controllers connected in parallel. The range of pressures to be measured extends over 12 decades, i.e. from 10^{-7} to 10^5 Pa . Such a large pressure interval can be covered only by the use of various instruments with overlapping pressure ranges (see [1] for details). The gas pressure is measured in the lower part of the test vessel, 410 mm below a LN-cooled baffle. The measuring gauge tube is linked with the vessel by an aperture. The pumping speed is determined according to the flow meter method using the PNEUROP standard dome and it is derived as a quotient of throughput and pressure during the gas-admitting phase. Thus, the measured pumping speed can be expressed as a function of the gas load or the pressure during pumping, respectively.

Various measurements of the pumping speed for the pure gases (helium, hydrogen and its isotopes protium and deuterium) were carried out at the TITAN facility for the two panel arrangements mentioned above. The gas load on a panel was gradually increased by increasing the flow rates in a stepwise manner. The comparison of the pumping speed evaluated from the experimental results as a function of the gas load on a panel revealed discrepancies depending on the panel geometry. In particular, the specific pumping speed for the quilted panel was found to be significantly smaller (by a factor of 2.95) than the corresponding one for the circular panel.

The pumping speed of the TITAN structure depends in a complex manner on the admittance rate of the gas, the pumping characteristics of the system and the cold surface, the type of sorbent used, the temperature and the gas load. Therefore, it became necessary to assess the impact of all these factors, including the geometry of the entire experimental facility on the pumping speed. The influence of flow rate and flow regime as well as of the temperature on the panel pumping performance was discussed extensively in [3]. The present study is exclusively concerned with the

quantitative evaluation of the geometry impact on the pumping characteristics of the TITAN facility.

The TITAN experimental setup operates in the molecular and in the transition flow regimes. The molecular flow exists at pressures lower than 10^{-3} Pa at the pump inlet. In such rarefied state of a gas (Knudsen number $Kn \gg 1$), the gas particles (atoms and molecules) virtually interact with the wall only and not with each other. For this reason, the kinetic theory of an ideal gas creates a sufficient basis for the theory of molecular flow. In the model of ideal gas, the particles are considered as point masses, exerting no force upon each other and merely colliding elastically with the structure walls. The physical properties of a gas at rest, such as pressure, density, temperature, specific heat capacities can be described quantitatively using the Maxwell distribution function for the particle velocity. For the analysis of gas flows at the macroscopic or molecular level, the Boltzmann equation with a vanishing collision term provides an adequate mathematical model. At a lower degree of gas rarefaction ($Kn \ll 1$), the intermolecular collisions must be taken into account additionally. Therefore, in case of the transition flow regime the discrete particles or molecular model is governed by the general Boltzmann equation with a non-zero collision term. The Boltzmann equation is not amenable to analytical solution for non-trivial problems, and it causes overwhelming difficulties for conventional numerical methods. However, the discrete structure of the gas at the molecular level enables to overcome these difficulties through direct simulation of the physics of the flow rather than mathematical modelling.

In the absence of intermolecular collisions, collision-less flow fields may be formed by superimposition of a free stream and the reflected molecules, involving multiple reflections from a surface. This class of problem is ideally suited for a probabilistic method called the test-particle Monte Carlo method. The great advantage of the Monte Carlo method is that it provides an efficient technique for studying the molecular gas flow in arbitrary complex vacuum structures. The Monte Carlo approach was chosen to predict the behaviour of a TITAN pumping system and successfully applied to analyse its pumping characteristics.

Monte Carlo simulations of the particle flow in the TITAN structure were carried out with the existing general-purpose Monte Carlo code MOVAK3D [4]. An objective of the simulations was to deliver an estimate for the loss in pumping speed due to the combined effects of the different TITAN structural components taking into account their actual geometry.

2 Estimation of integral characteristics of a vacuum system by the Monte Carlo method

The test-particle Monte Carlo method for the analysis of collision-less flow in vacuum systems involves the setting up of a mathematical representation of the vacuum structure to be studied, the attributing of physical properties to each component of the structure and then the using of a fast computer to simulate the history, i.e. the behaviour of a large number of gas molecules within the structure. This procedure which involves multiple surface reflections is based on tracing the trajectories - random walks- of individual molecules from the point of their introduction into a given structure to the point of their leaving the structure or being captured by a surface within the structure. The probability of a molecule passing through a structure or being captured depends on its initial direction at the entry surface, on the direction into which it is scattered at any intersection point with the internal walls and the absorption rate. In particular, this probability is independent of molecular speed and there is no need to consider the distribution of this quantity. From the recorded number of interactions of the molecules with each surface element (so-called scores) the basic integral characteristics of the vacuum system can be evaluated [5]:

- The transmission coefficient which defines the probability that the particle, passing through the inlet opening of the structure exits through its outlet opening and is equal to the ratio of the number of outgoing to the number of incoming particles
- the backscattering coefficient which defines the probability of emergence in the reverse direction from the part under consideration and is equal to the ratio of the number of molecules backscattered to the inlet opening to the number of molecules which have entered the structure
- the capture coefficient which defines the probability that a particle incident at a reference cross-sectional surface of a structure will be captured by the cryosurface and is numerically equal to the ratio of the number of molecules which were captured, i.e. remained in the structure, to the number of molecules that have entered.

These three coefficients can be estimated using scores, based on a suitable amount of histories sampled during the course of the simulation. The costs of the computation of 10^5 or 10^6 particle random walks are negligible, such that a four-figure accuracy is obtained readily. Another advantage of the Monte Carlo method is the ease, by which it is able to deal with a very complex flow geometry. Thus, the

pumping characteristics of an arbitrary complicated geometrical structure can be evaluated from the simulation results.

A PASCAL implementation of this method, called MOVAK3D [6], originally written to support the geometrical optimisation of the vacuum ducts of fusion reactors, has been applied here to analyse the TITAN experimental facility.

3 An overview of the Monte Carlo Code MOVAK3D and its main features

The Monte Carlo code MOVAK3D requires a detailed geometry specification of the structure, a definition of the physical properties of each surface and an appropriate set of parameters increasing the efficiency of the simulation run. MOVAK3D treats an arbitrary three-dimensional configuration which, however, must be suitably decomposed into the pre-defined elements [6]: Triangles, parallelograms, circles, squares with hole, hexagons and octagons with hole or so-called units: Pipe, elbow, cold trap, tapered pipe and branching pipe. To these basic geometry elements the surfaces of revolution, such as spheres, cylinders, cones and rings can be attached by a circular ring or another joining element with a hole.

To every specified surface one of the following physical properties must be assigned: Source (point, surface, isotropic or anisotropic including a beam source), absorber (black or grey), diffuse scatterer (with a cosine distribution of the emitted particles), a mirror-like reflector. Additionally, the structure may be subdivided by the control surfaces into exclusive volumes which enable to check the local molecular flow, to calculate relative pressures and to reduce the computational time. In the course of a simulation, MOVAK3D randomly chooses among the specified sources the first and the subsequent source surfaces, the spatial coordinates of the source particle emission and its flight direction. To each source particle an appropriate weight is assigned. Then, the possible collision point with the nearest wall is calculated, assuming that the particle path is piecewise linear. Intermolecular collisions are not taken into account.

The implemented models for the gas-surface interactions are based on diffuse, specular and a simplified accommodation model. Specular reflection is perfectly elastic with the molecular velocity component normal to the surface being reversed, while those parallel to the surface remain unchanged. In the diffuse reflection the velocity of each molecule after reflection is independent of its initial velocity. However, the velocities of the reflected molecules as a whole are distributed in accordance with the Maxwellian distribution for molecules that are directed away

from the surface. Equilibrium diffuse reflection requires both the surface temperature and the temperature associated with the reflected gas to be equal to the gas temperature. In the case of specular reflection, the gas may have a stream velocity parallel to the surface, and a specularly reflecting surface is functionally identical to the plane of symmetry. The accommodation model represents the most common generalisation of the diffuse model so far, as the incident and reflected molecules are allowed to have different temperatures. An indication of the extent, to which the reflected molecules have their temperature adjusted towards that of the surface is given by the thermal accommodation coefficient. The range of the accommodation coefficient extends from zero for no accommodation to unity for the complete thermal accommodation. In this model, the non-diffuse reflection is represented by assuming that some fractions of the molecules are reflected specularly, while the remainder is reflected diffusely. However, this model cannot reproduce the molecular beam data that have been obtained for particular cases [7] and there is no justification for the implicit assumption that the result should lie between the limits set by complete diffuse and complete reflection. Therefore a more general empirical model is needed.

If the particle impinges on an absorbing surface, it may be fully or "partially" absorbed. In the latter case, the particle weight is reduced and the amount of reduced weight is attributed to the particle weight deposited on the surface. This procedure may lead to a very small particle weight, practically not giving any significant contribution to the final result. Tracing such particle further on would extend enormously the computational time on one hand and increase the variances on the other. Therefore, the Russian roulette option was made available to eliminate such cases from the further considerations by removing a particle or doubling its weight. The amount of particles to be considered in one simulation run is problem-dependent. Care must be taken regarding the sufficient accuracy of the final results, since they have a statistical nature and are biased with a statistical uncertainty (see chapter 9). The MOVAK3D code yields an output list with the balance table, containing the deposited particle weights for each absorbing surface.

A serious drawback of the program is the separate determination of the particle path in the global and local Cartesian coordinate system. The local coordinates are superimposed when surfaces of revolution are incorporated in the geometrical model in order to simplify their mathematical description. If the model contains surfaces of revolution, the definition of the reference plane for the local coordinate system is required. The normal to the plane must be collinear with the axis of rotation. When both the flat surfaces and the surfaces of revolution are used, the tracing of a particle is interrupted on the reference plane. The particle random walk (which may be described in an arbitrary geometry) begins on the source side as seen from the

reference plane. The particle pathway is recorded up to a common cross-section control surface lying on the reference plane. As soon as a particle crosses this surface, its intersection point coordinates and directional vector components are transformed to a new coordinate system. They serve as the initial point and direction for further particle tracing in the forthcoming geometry. An inverse transformation of the new generated pathway is not done; thus, the reference to the previous coordinate system is lost completely. This strategy was adopted to save storage area. However, it implies a severe limitation to the geometry description: The flat surfaces like parallelograms and triangles cannot be embedded into any solid of revolution. This was the main reason why it was decided to depict the whole geometrical structure of TITAN in global Cartesian geometry, representing cylindrical surfaces as prisms with an octagonal cross-section. It was proved that this approximate treatment of the structure geometry has no significant influence on the final results.

In MOVAK3D, only one type of gas particles can be considered in one simulation run. This means that gas mixtures cannot be treated explicitly. Nevertheless, in many cases the behaviour of a gas mixture can be predicted by simulating the flow of each mixture component separately and then summing up the results in an appropriate way. This method, however, has a limited range of application, since the absorption rates for the different gas components must be independent of each other.

Gas-gas interactions are not simulated, as a gas velocity distribution is not modelled. A radiation heat load on surfaces may be predicted by considering the generated particles as photons and all surfaces of the structure as fully absorbing sources with the emission density proportional to the emission density of a black radiator ($\sim T_{\text{surface}}^4$, where T denotes the temperature of the surface). The weight of particles deposited on a particular surface will then be proportional to the thermal load transmitted to the surface, whereas the particles emitted from each surface give an estimation of the energy losses.

4 Geometrical model of the TITAN structure for the analysis with MOVAK3D

The layout of the TITAN facility is shown in Fig. 1. The corresponding geometry model of the TITAN structure created for the MOVAK3D code is illustrated in Fig. 2. The model structure consists of four components: The PNEUROP dome, a baffle and a cryopanel embedded into an 80K volume. Comparison between the original and the model structure shows that all relevant TITAN components that have a strong impact on the flow of gas molecules through a system were taken into account. The

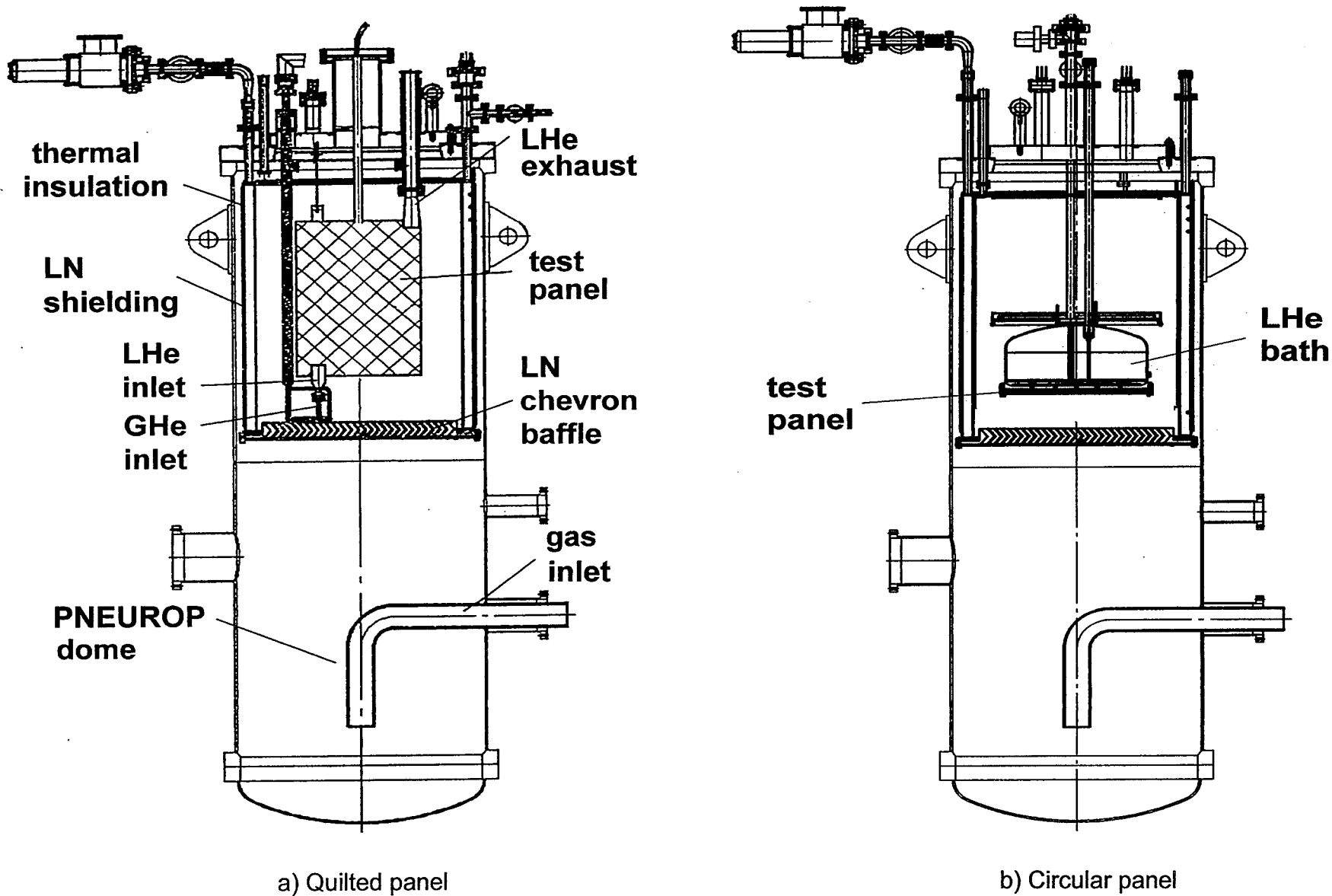


Figure 1. Low-temperature adsorption facility TITAN with two different test panels.

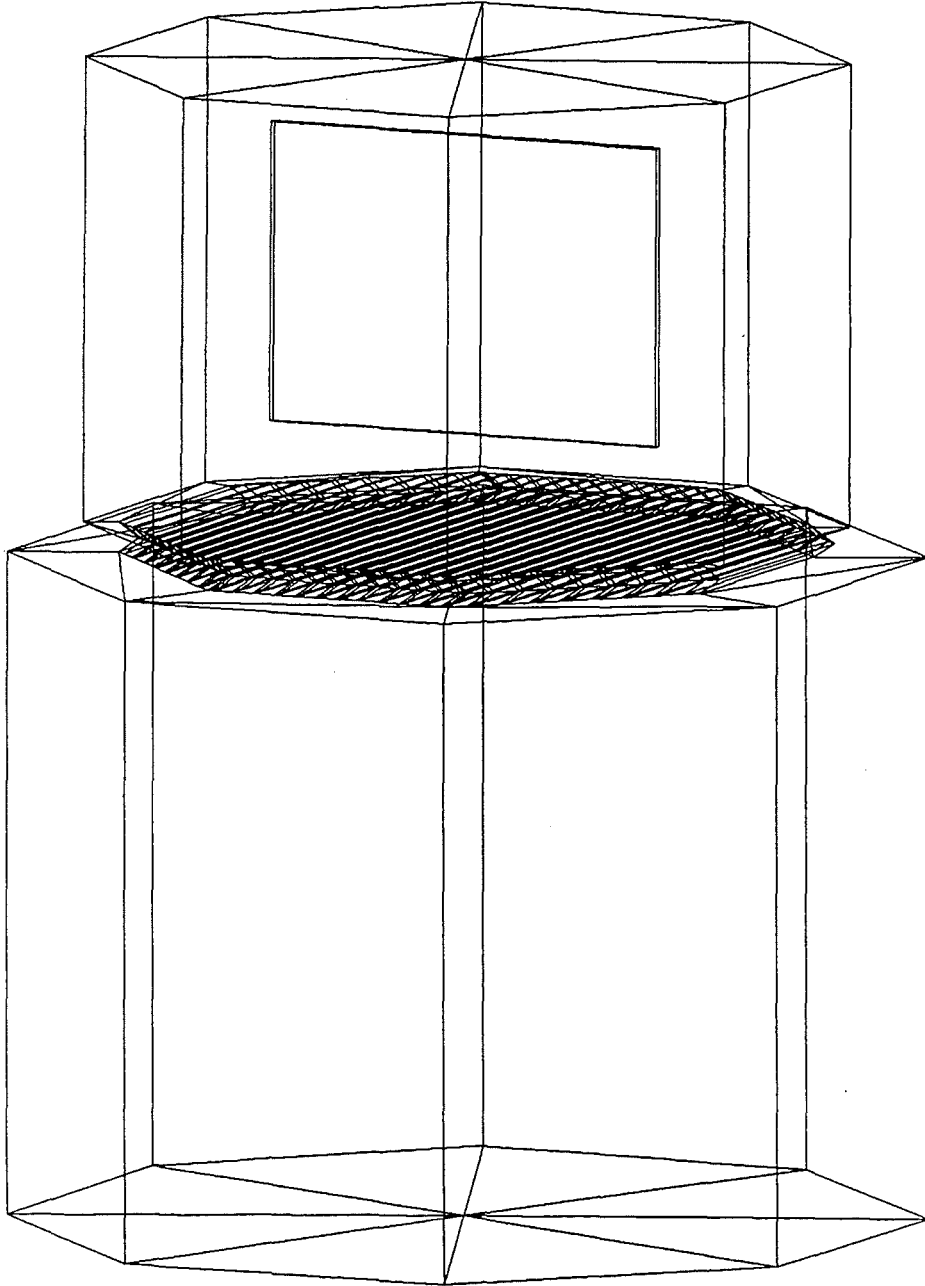
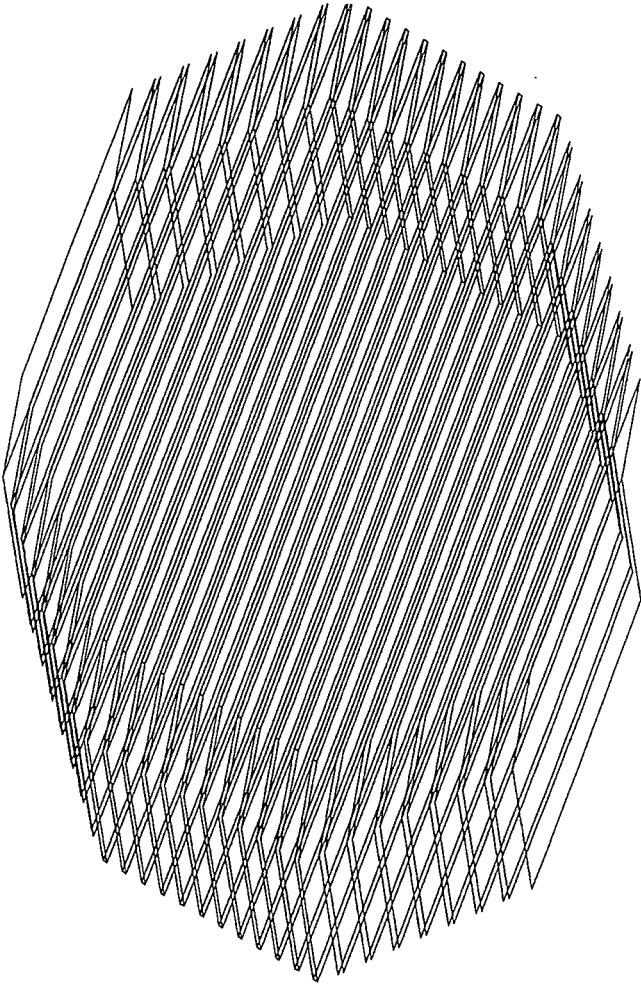
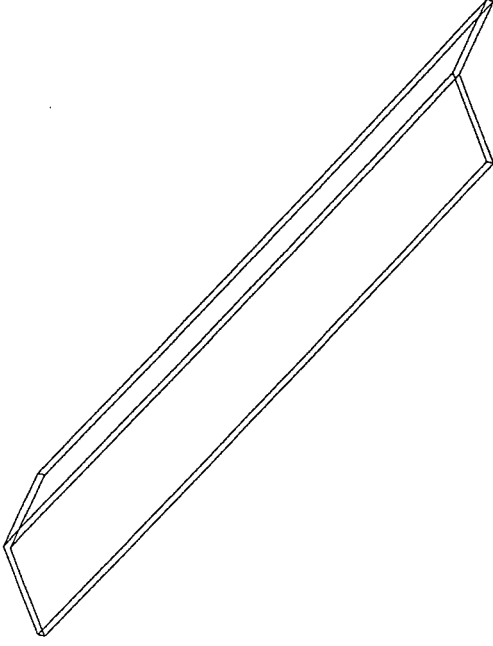


Figure 2. Geometry model of the TITAN facility with the quilted panel in the MOVAK3D code.



a) Entire baffle



b) One V-shaped plate

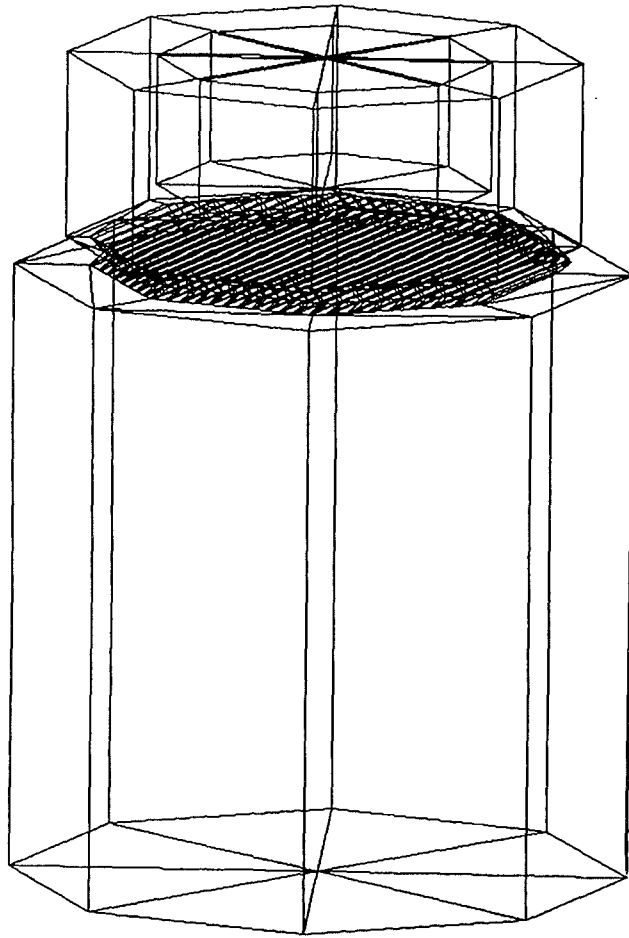
Figure 3. MOVAK3D representation of the chevron baffle.

chevron baffle throttles the conductance to the pump and, hence, influences significantly the pumping performances of the whole system. A cryopanel with its peculiar sticking coefficients for different gas species obviously determines the overall pumping probability. Finally, due to the external arrangement of the ionisation gauges connected to the test vessel and a reduction of the passage area between the PNEUROP dome and the baffle, the segment of the PNEUROP dome must be considered additionally.

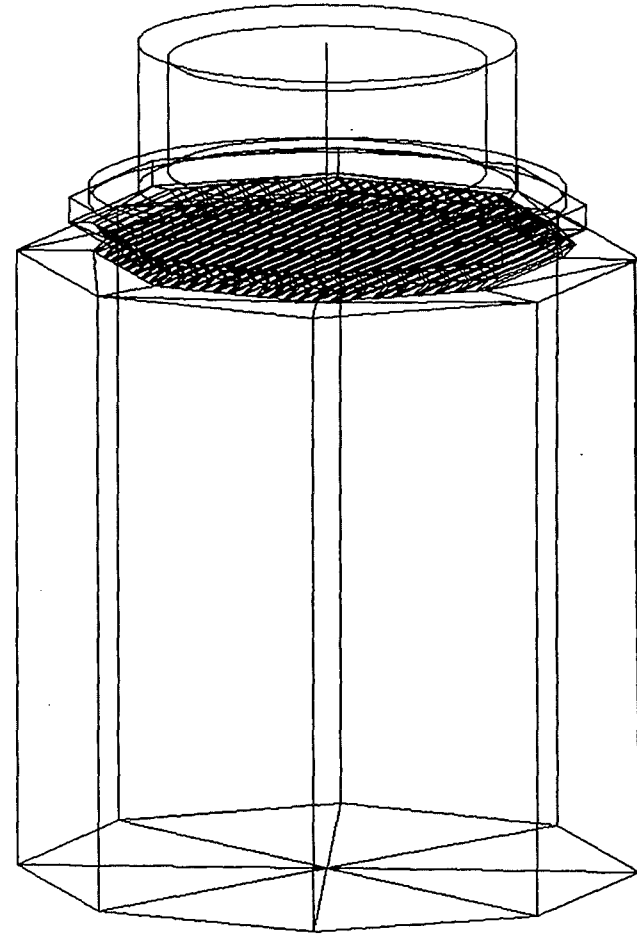
The upper segment of the PNEUROP dome (diameter $D=700$ mm, height $H=410$ mm) was included into the MOVAK3D model. It was represented as a channel with an octagonal cross-sectional area. The particle source was located at the segment bottom. Thereby, the reference plane for the pumping speed determination was placed exactly at the height where the pressure is measured. It was assumed that the spatial distribution of gas particles emitted from the source surface is uniform and the angular distribution of particle emission direction is isotropic.

The chevron baffle had to be modelled quite precisely in order to achieve a proper estimation of its conductance. The chevron baffles are opaque for light rays transmitted on a straight line in any direction, i.e. no molecule can pass through them without colliding with the walls of their internal structure. The baffle consists of straight V-shaped plates, inclined at an angle of 53° to the vertical (Fig. 3a) and spaced from each other by a distance of 19 mm. The plates cross the circle of their enclosure; thus, their lengths differ with their positions. The diameter of the baffle opening is 527 mm, the baffle thickness is 50 mm and the wall thickness of the V-profiles is 3 mm. In the MOVAK3D model an equivalent octagonal baffle enclosure replaced the circular one. The plate lengths were adequately determined via a FORTRAN program, additionally written for this purpose. Thus, 26 V-profiles of varying length could be included into the model of the baffle (see Fig. 3b). The shape of each plate is reconstructed using 10 parallelograms. They are orientated in such a way that only the external surface of the plate can diffusely reflect impinging gas molecules.

An important component in the assembly is the cryopanel. The test panel in quilted design has the dimensions 500 mm \times 350 mm, which roughly corresponds to the panel geometry foreseen for the prototype pump. The test panel is modelled as being composed of six parallelograms: The first two represent the panel front and the rear surface, and the remaining four, significantly smaller, the other boundary surfaces. In the determination of the panel thickness, the copper layer, the sorption material layer and the bonding cement were taken into account. All six surfaces are considered to



a) Parallelograms



b) Parallelograms and surfaces of revolution

Figure 4. Geometry model of the TITAN facility with the circular panel in the MOVAK3D code.

be absorbers. The quilted geometry was neglected in the MOVAK3D model. The cryosorption panel is embedded into the centre of the 80K volume.

The 80K environment is simulated in MOVAK3D by a prism with an octagonal cross-section (radius of an inscribed circle 582 mm, height 678 mm) closed from the top. Thus, 8 parallelograms and 8 triangles bound the 80K volume. Inward orientated sides of the walls are defined as diffuse reflectors.

The four components described above were put together in a series arrangement. In this sequentially connected set, the cross-sectional area of the baffle is smaller than both the cross-sectional areas of the PNEUROP dome and of the 80K volume. To reproduce the structure of the TITAN facility, 441 spatial points, 104 triangles and 198 parallelograms were needed.

For the TITAN facility with a circular panel two different MOVAK3D representations were developed (see Fig. 4). The first included the surfaces of revolution, whereas the second one consisted of flat surface elements only. The aim of this apparent redundancy was to estimate the influence of the geometrical representation on the calculated system characteristics. It occurred to be negligibly small.

5 Specification of the computational task

The measurements in TITAN are related to the vacuum chamber, thus, the measured pumping speed represents the effective pumping speed and not the net one related to the pumping cryosurface. Since a series of components is inserted between the panel and the vacuum chamber, the pumping speed S over the chamber must drop as compared to the corresponding pumping speed value S_p over the pump.

If the conductance C is added to a system with a known pumping speed S_p , then by means of the well-known reciprocal addition equation [8]

$$\frac{1}{S} = \frac{1}{S_p} + \frac{1}{C} \quad (5.1)$$

is obtained.

This equation can be expressed in another form as

$$\frac{S}{S_p} = \frac{C}{S_p} \left[1 + \frac{C}{S_p} \right]^{-1} \quad (5.2)$$

which shows explicitly the decrease of the pumping speed ratio S/S_p due to the ratio C/S_p between the conductance of the system and the pumping speed of the pump. This relationship is represented in Fig. 5. It can be seen that when the values of the conductance and of the pumping speed of the pump are equal, only 50% of the pumping speed are exploited in the vacuum vessel. In order to use 80% of the pumping speed, the ratio C/S_p must be 4, while for the ratio $C/S_p=0.1$ only 10% of the pumping speed of the pump are utilised in the vacuum enclosure. This implies that if the conductance of the components introduced between the panel and the vessel is the factor limiting the pumping speed, enlarging the pumping panel area will bring no advantage.

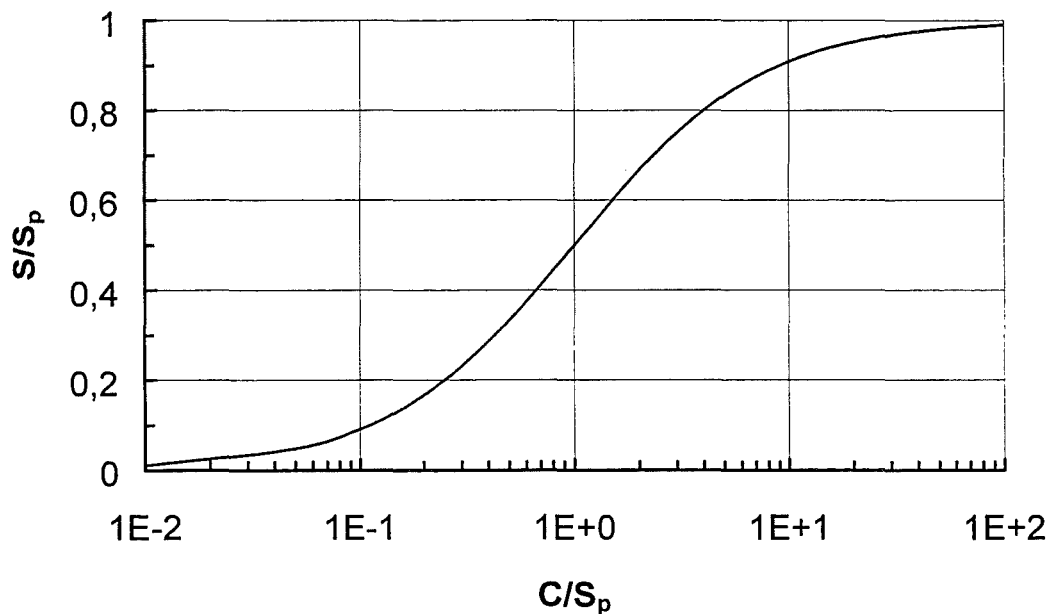


Figure 5. S/S_p as a function of C/S_p .

Conductance and pumping speed are associated with the description of gas flows in volumetric terms [9]. This is convenient for the basic computations, if the heat transfer effects are negligible and the gas quickly accommodates to the temperature of the vessel or a pumping duct. The mass flow can be measured in units of throughput Q such as mbar·l/s at a fixed temperature. Throughput simply is a product of the pressure p and the volume flow of the gas S for any given location (cross-sectional plane) in the flow passages.

$$Q = p \times S \quad (5.3)$$

Two distinct geometries exist, in which the flow parameters are mutually associated as in Eq. (5.3),

- the orifice geometry

and

- the pipe flow geometry.

In case of the orifice, the pressure is measured far away from the orifice. The gas flow conductance of the orifice is an inverse measure of its resistance to the flow and determines the pressure drop at a given mass flow:

$$C = \frac{Q}{\Delta p} \quad (5.4)$$

$$\Delta p = p_1 - p_2$$

where p_1 and p_2 are upstream and downstream pressures, respectively. If p_2 is much smaller than p_1 , we may speak of the orifice speed

$$S = C = \frac{Q}{p_1} \quad \text{when} \quad p_1 \ll p_2 \quad (5.5)$$

As already mentioned, p_1 is not associated with the vicinity of the orifice, but with an upstream location where the gas conditions may be considered to be isotropic.

In the case of pipe flow, pressure and speed are related to the same cross-sectional plane. In molecular flow, the conductance of the pipe is defined as the flow through the pipe divided by the differential pressure across the pipe. When a conductance is physically measured in the experiment, it is normally done by placing the component between two large volumes and measuring the flow as well as the pressure in both volumes. This conductance determination includes the pressure drop across the pipe as well as the pressure drop across the exit. Thus, corrections must be made to account for these pressure differences.

The TITAN structure combines both types of geometry. The components of TITAN are connected in series. The resulting complex pumping system has sections with

decreasing as well as with increasing cross-sectional areas. Thus, care must be taken in calculating the total conductance. It has long been recognised that the conductance of the component itself depends not only on the geometry of that component, but also on the geometry of the adjacent components. In particular, a conductance of a baffle depends on whether it exits to a large volume, to a component having the same diameter or to a component with an intermediate diameter. Therefore, it is important to determine the conductance of the entire structure of the TITAN facility rather than to combine the conductances of its single components using the addition theorem of reciprocal conductances. This can be done only by the Monte Carlo method.

The conductance depends on the arrangement and the dimensions of structure components on one hand and on the type and temperature of the gas on the other. In the molecular flow regime, the conductance is theoretically characterised by the transmission probability. The transmission probability w represents the fraction of molecules entering and actually passing through the structure. A fraction $(1-w)$ of incident particles is scattered back and leaves the structure through the entrance surface. The aim of the MOVAK3D calculations is to obtain a quantitative estimation of the influence of structure geometry on the conductance. This is achieved by the determination of the transmission probability of the apparatus up to the upper section of the 80K volume containing the panel.

The pumping effectiveness of the TITAN structure strongly depends on its overall capture probability. The knowledge of the capture probability is especially useful in practical considerations, since it allows to associate the pumping speed S of the whole system (i.e. the measured quantity) to a suitably chosen reference cross-sectional area. The capture probability accounts for the actual structure geometry as well as for the pumping performance of the panel. It comprises the gas sticking coefficient defined as the probability that an incident gas molecule remains on the panel surface.

Cryosorption pumps are not continuous-throughput pumps. The pump gas is not exhausted to the atmosphere, but kept inside the pump. The gas remains in the pump either as a thin film (one or a few monolayers thick) having the density of a liquid or as a deposit resembling snow or frost. It may also be sorbed inside the pores of the sorbent material or at its outer surface. Because of saturation effects, the pump has to be regenerated or degassed occasionally. The amount of the pumped gas and the required period between regeneration govern the design at the extreme ends of the vacuum pressure scale. In the TITAN facility the pumping surfaces provided have to pump down different gases, some of which are pumped as

a result of condensation and some due to sorption. In particular, for helium which is pumped by sorption, the pumping speed will decrease as the surface coverage increases. The pumping speed depends on the arrival rate of the gas, the capture probability and the area of the cold surface. The arrival rate of the gas in turn depends on its molecular weight and temperature. Moreover, the pumping speed for helium will also depend on the amount of previously pumped gas on a surface. The pumping speed for a gas mixture may not only depend on the total amount of previously pumped gas, but also on the sequence, with which different gases have been introduced into the pump (i.e. the loading history). Thus, for the analysis of the TITAN pumping system performances, the following factors are of primary importance:

1. Conductance of the whole TITAN vacuum structure and its constitutional parts. It is to be determined on the basis of the calculated transmission probabilities.
2. Capture probability which permits to express the pumping speed as a function of the gas sticking coefficient, cryosurface area and the conductance.
3. Fluctuation of the gas pressure within the system.
4. The influence of the geometry of the cryopump on the pumping speed. In particular, the dependence of the capture probability on the panel incline with respect to the gas flow direction.

The analysis of the cryopanel pumping performance should additionally comprise:

1. Evaluation of the sticking coefficients of the panel from the experimental data and the calculated transmission and capture probabilities
 - for the quilted panel
 - for the circular panel
2. Numerical investigation of the saturation point of helium pumping, employing the MOVAK3D special modelling option which allows to account for decreasing sticking coefficients with increasing gas load on the panel.

6 Presentation and discussion of the Monte Carlo simulation results

In the MOVAK3D simulations, the entrance area (eight triangles representing an octagonal cross-section of the PNEUROP dome) was defined as a source surface window with a uniform spatial distribution of emitted particles and an isotropic 2π distribution of their flight directions. The vacuum boundary conditions were imposed, i.e. the backscattered particles which cross the entrance area while leaving a system cannot return to it. For particles that are reflected from the walls, a cosine reemission distribution was chosen, with the reflection coefficient equal to 1. At pressures below 10^{-3} Pa and at the temperature 293K, the mean free path of H_2 and He, is larger than 1 m and, thus, exceeds the dimensions of the system. Therefore, the mean free path of the gas molecules was set to infinity for the calculations.

6.1 Pumping system characteristics

Part of the Monte Carlo simulations performed was devoted to the estimation of integral characteristics of the TITAN pumping system and its constitutional parts. The fundamental property of the integral characteristics is the universality which they provide for the quantitative description of vacuum-system components. This property facilitates the formal mathematical approach and the interpretation of experimental results.

6.1.1 Transmission probability

For the transmission probability calculation, an open structure with an inlet area A_{dome} and an outlet area A_{pump} was considered. In accordance with the vacuum boundary conditions, both the inlet and the outlet were defined as absorbing surfaces with an absorption rate, denoted a , equal to 1. This assumption corresponds to the nature of the problem. Particles which cross the outlet area cannot come back into the system, they are lost, i.e. eliminated by absorption on the outlet surface.

The transmission probability w for the whole TITAN vacuum structure with the inlet A_{dome} at $z=700$ mm and the outlet A_{pump} at $z=1312$ mm (i.e. from the pressure measurement level up to the panel) calculated with MOVAK3D for 200 000 particles amounts to 0.1. The estimated intrinsic transmission probability of the chevron baffle is 0.19.

6.1.2 Capture probability

For the determination of capture probability the entire structure including the pumping surface must be investigated. The panel removes the gas molecules by cryosorption and/or cryocondensation with a specific pumping speed depending on the sticking coefficients. Hence, in the MOVAK3D input model the panel surfaces must be defined as black or grey absorbers. The pumping characteristics of the panel are considered through the absorption rate "a", which represents the gas sticking coefficient. The absorption rate depends on the type of gas pumped. It can be regarded as a constant over the whole simulation run, as in case of hydrogen isotopes, the sticking coefficient of which remains constant during the whole pumping process. This assumption, however, is no longer adequate when helium is pumped, since the sticking coefficient for helium is decreasing with increasing gas loads. To take this into account, the absorption rate must be expressed as a function of the relative molecular coverage on the surface.

The capture probability c is defined as the ratio of the amount of particles fixed by the adsorbing surface to the amount of particles impinging on the previously chosen reference surface lying within the structure. The sticking coefficient α is the ratio between the number of particles sticking to the cryosurface and the number of particles impinging on it. The difference between the capture probability and the sticking coefficient becomes apparent when noticing the fact that the sticking coefficient characterises the interaction between the gas molecules and the cryosurface only, whereas the capture probability refers to the whole structure containing the cryosurface as its component. Therefore the capture probability must be a function of both, the sticking coefficient which becomes equivalent to an absorption rate of the panel surfaces in the considered MOVAK3D simulations and the transmission probability of the system.

Fig. 6 shows the capture probability c for different values of the sticking coefficient. They were obtained by performing six independent computational runs with 10 000 histories each. As expected, the capture probability reaches its maximum value for $\alpha=1$. For smaller absorption rates of the panel surface the capture probability also decreases until it vanishes for $\alpha=0$.

The maximum capture probability calculated from 200 000 histories for the structure with a quilted panel amounts to 0.0915, whereas for the structure with a circular panel the corresponding value is 0.085. The smaller capture probability for the latter is caused by the smaller cryosurface area as compared to the area of the quilted panel and the gap between the panel boundary and the walls of the 80K shielding. Due to the gap, gas molecules can pass to the upper part of the 80K volume and

the gap, gas molecules can pass to the upper part of the 80K volume and from there, after multiple reflections, they are partly scattered back to the PNEUROP dome.

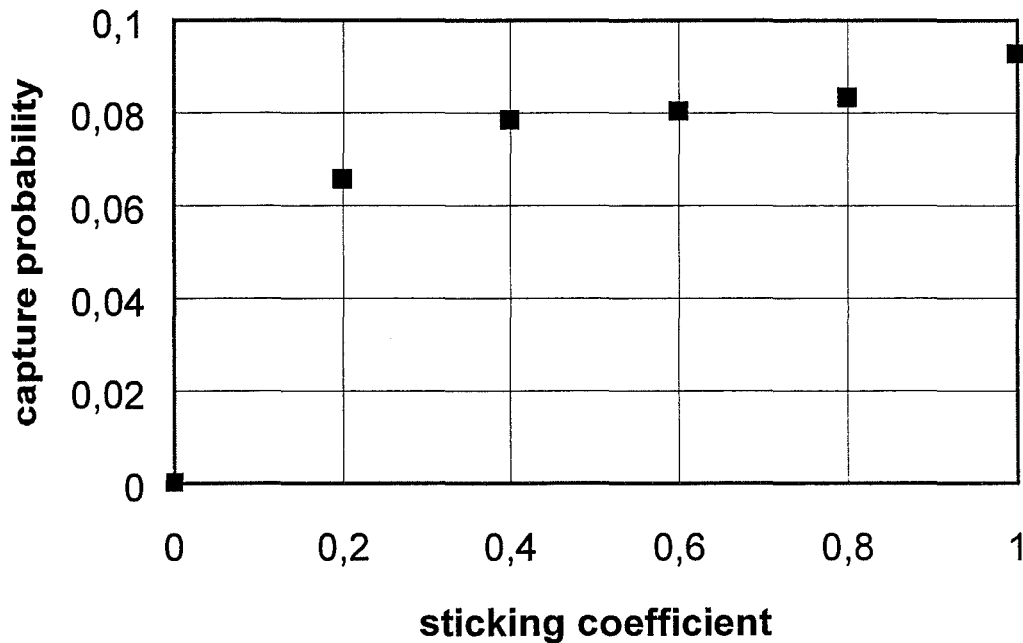


Figure 6. Capture probability of the TITAN structure versus the gas sticking coefficient.

6.2 Conductance

The conductance C depends on the structure shape (through the transmission probability w), on its inlet cross-sectional area (A) and on the type and temperature of the gas. In the molecular flow regime the conductance is independent of the pressure and is given by [10]

$$C = A w \frac{v}{4} \quad (6.1)$$

whereas in our case: $A = A_{\text{dome}}$;

$v/4$ is the x-component of the average gas velocity, as derived from the Maxwell distribution

$$\frac{v}{4} = 36.38 \sqrt{\frac{T}{M}} \quad [\text{m/s}] \quad (6.2)$$

T is the gas temperature in K

M is the molecular weight (in g/mol)

Since the conductance depends on velocity, it will vary with the species of gas (molecular weight) and temperature proportionally to $(T/M)^{0.5}$. The value $v/4$ is numerically equal to the surface-related volume flow rate \dot{V}/A which passes through a reference surface or to the maximum surface-related pumping speed S/A of an (ideal) pump for the gas having the temperature T .

6.3 Net pumping speed

The effective pumping speed S can be expressed as the maximum pumping speed related to the entrance area A_{dome} multiplied by the capture probability c . The panel pumping speed S_p is the maximum panel pumping speed multiplied by the sticking coefficient α (see [10])

$$S = c A_{\text{dome}} \frac{v}{4} \quad (6.3)$$

$$S_p = \alpha A_{\text{panel}} \frac{v}{4} \quad (6.4a)$$

Thus,

$$S_p = \frac{S}{1 - \frac{S}{C}} \quad (6.4b)$$

Eqs. (6.3) and (6.4a) combined with Eqs. (5.1) and (6.1) give

$$\frac{1}{c A_{\text{dome}} \frac{v}{4}} = \frac{1}{\alpha A_{\text{panel}} \frac{v}{4}} + \frac{1}{w A_{\text{dome}} \frac{v}{4}} \quad (6.5)$$

If it is assumed that the temperature of all TITAN structure units is constant, the influence of the geometry on the pumping performance can be studied directly. Uniform temperature implies a constant x-component of the mean gas velocity in the whole structure.

Thus,

$$\frac{1}{c} = \frac{A_{\text{dome}}}{A_{\text{panel}}} \times \frac{1}{\alpha} + \frac{1}{w} \quad (6.6)$$

$$c = \frac{\alpha}{D + \frac{\alpha}{w}} \quad (6.7)$$

$$D = \frac{A_{\text{dome}}}{A_{\text{panel}}}$$

Eq. (6.7) combines the losses of the pumping speed due to the geometry (w and D) and the pumping probability of the panel (α) with the common quantity c . Therefore, it quantifies the impact of the whole TITAN structure on the pumping speed. It allows to calculate explicitly the capture probability for a given sticking coefficient and a known transmission probability of the structure. In particular, for the TITAN facility with the quilted panel:

$$c = \frac{\alpha}{1.0996 + 10\alpha} \quad (6.8)$$

Eq. (6.8) delivers an excellent reliability check of the MOVAK3D code. Thus, it is interesting to make a direct comparison between the estimated capture probabilities (MOVAK3D) and the analytically calculated exact values. This is illustrated in Fig. 7.

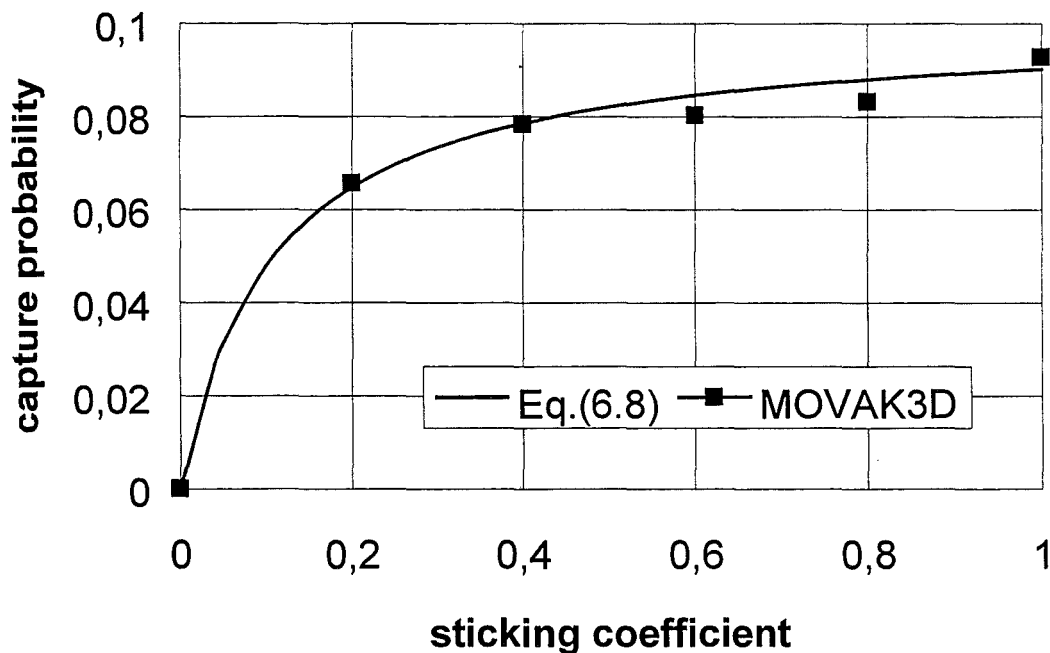


Figure 7. Comparison between the capture probability calculated from Eq. (6.8) and MOVAK3D results.

The agreement is very good within the uncertainty limits of the Monte Carlo calculation.

The concepts outlined above are sufficient for basic interpretation of the pumping speed performance curves.

6.4 Relative pressure

The MOVAK3D code allows to introduce into the structure control surfaces which may serve to score particles crossing them and, thus, to control the local flow. The scores can be used to calculate the pressure in the vicinity of the control surface.

The incidence or particle flow rate density I , defined as the number of particles impinging on unit area of a surface in unit time, is given by [10]

$$I = n \frac{V}{4} = n(kT / 2\pi m_0)^{1/2} = p(2\pi m_0 kT)^{-1/2}$$

where $n=N/V$ denotes the particle number density and

m_0 the particle mass (in grams)

Consequently, the pressure on a surface is given by

$$p = I \cdot \sqrt{2\pi m_0 kT} \quad (6.9)$$

In accordance with (6.9), a ratio of pressures p_1 and p_2 measured on two differently situated surfaces A_1 and A_2 for an isothermal apparatus is

$$\frac{p_1}{p_2} = \frac{N_1 \cdot A_2}{N_2 \cdot A_1} \quad (6.10)$$

where N_1 and N_2 denote the number of particles impinging on a surface A_1 and A_2 , respectively. However, this procedure leads to the pressure dependence on the flow direction. In case this effect is not desired, it is advisable to use three control surfaces crossing each other at right angles at the point of interest within a structure.

Relative pressures were calculated for three different surfaces placed inside the TITAN structure at the high $z_1 = 1100$ mm, $z_2 = 1310$ mm and $z_3 = 1814$ mm, respectively. The first control surface was located under the baffle, the second inside the 80K volume right under the panel and the third just above the panel (see Fig. 8). Results of the MOVAK3D calculation performed by analysing 500 000 histories are comprised in Tab.1 and the corresponding relative pressure variation is illustrated in Fig. 9.

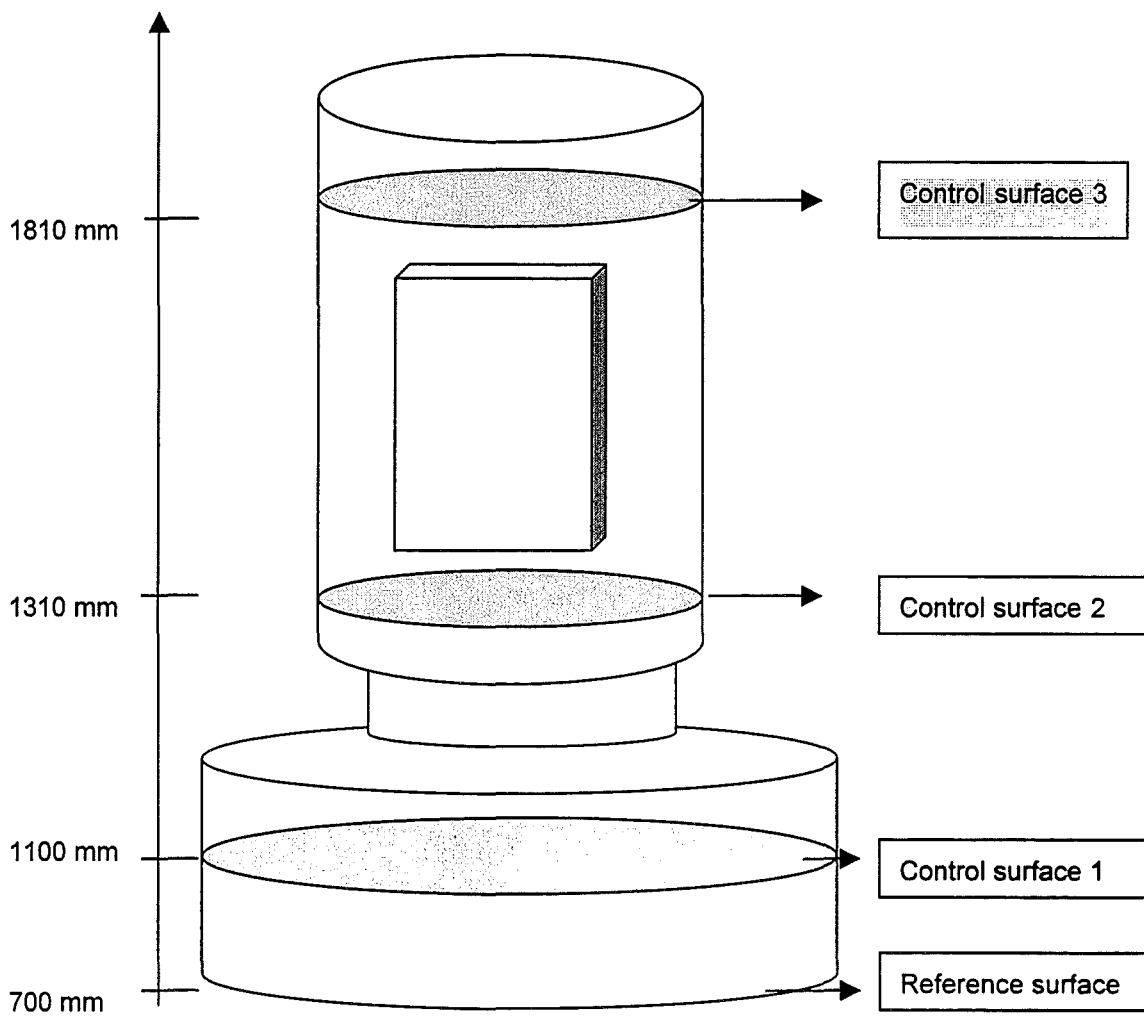


Figure 8. Location of the control surfaces in the TITAN facility for the relative pressure calculation.

Pressure ratio	Relative pressure
p_3/p_m	0.085
p_2/p_m	0.15
p_1/p_m	0.95
p_2/p_1	0.16
p_3/p_1	0.09
p_3/p_2	0.57

Table 1. Relative pressure derived from MOVAK3D results.

It can be seen that the pressure in the pump (on the 3rd control surface) decreases by one order of magnitude relative to the pressure in the PNEUROP dome.

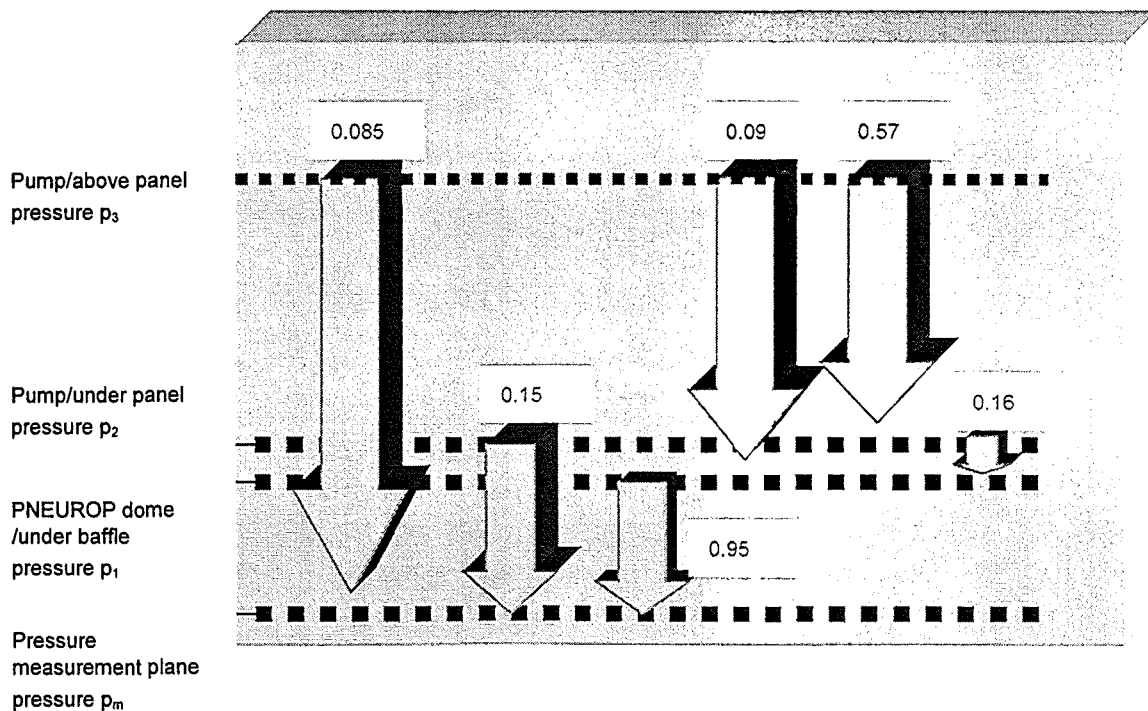


Figure 9. Fluctuation of the relative pressure in the TITAN pumping structure.

6.5 Capture probability depending on panel incline

A series of calculations has been carried out to investigate the effect of panel inclination with respect to the main gas flow direction. The objective of this study was to assess how the two panel sides contribute to the overall capture probability under different panel incline angles. The panel position was varied from the vertical arrangement to the horizontal one. The angle of inclination was changed from 0 to 90 degrees in 10 discrete steps (see Fig. 10). The sticking coefficient was chosen equal to unity in all simulation runs.

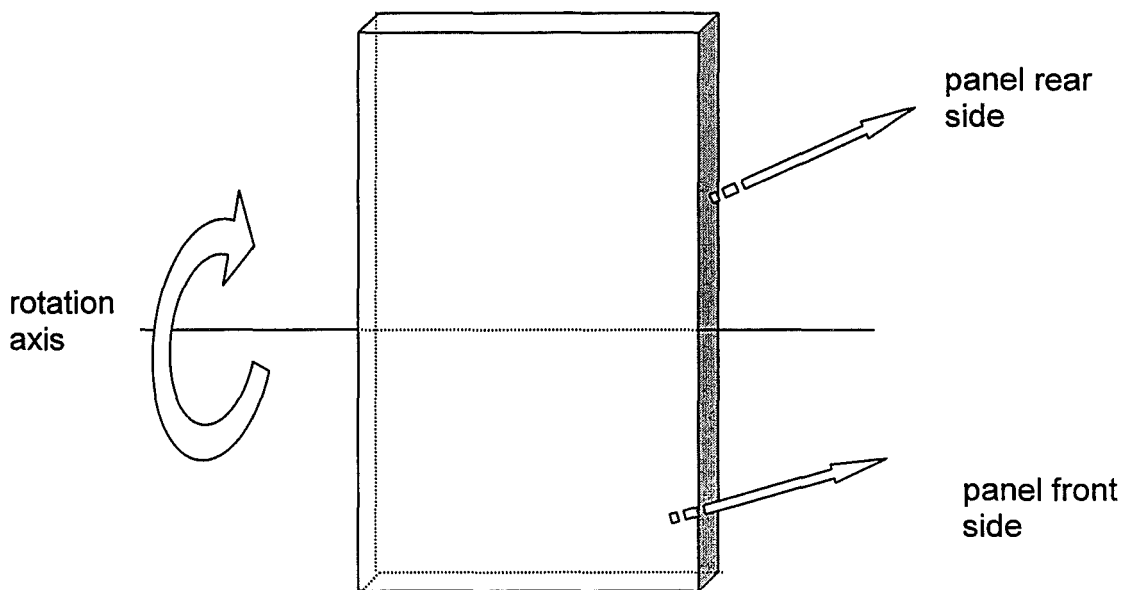


Figure 10. Schematic drawing of the cryopanel with the rotation axis.

In Fig. 11 the total capture probability obtained by simulating 100 000 histories is plotted versus the inclination angle of the panel. It can be seen that the capture probability of the TITAN geometry exhibits no discernible dependence on the panel configuration. However, the contributions by two different panel sides to the overall value differ significantly with the panel position. The number of gas molecules which may hit the rear decreases with increasing panel slope as depicted in Fig. 12. This can be utilised to optimise the pumping speed performance by trying to separate the gases by their adhesion mechanisms, keeping the front side of the panel uncoated and, thus, providing a condensation surface, and only coating the rear with sorbent material [11].

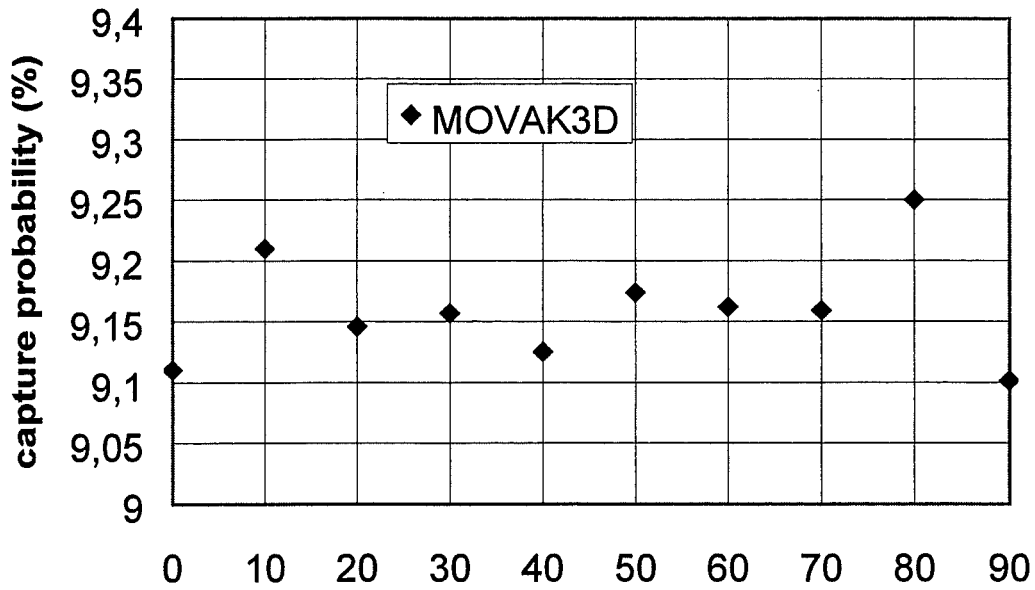


Figure 11. Overall capture probability versus panel incline with respect to the main gas flow direction.

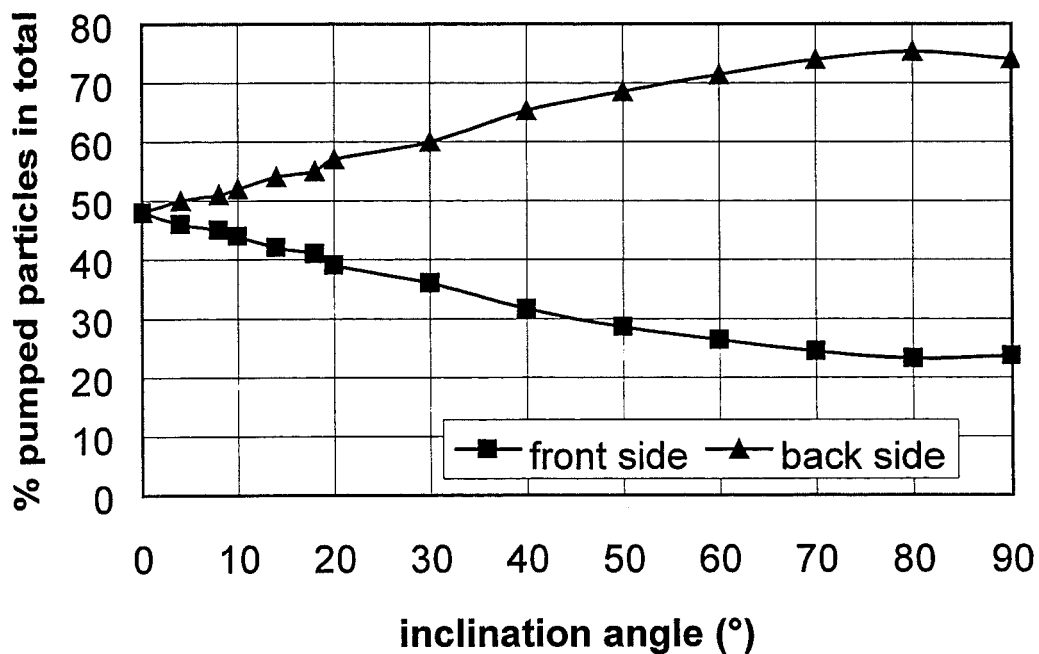


Figure 12. Contributions by the front and rear panel side to the overall capture probability.

6.6 Panel pumping performance

Gas molecules impinging on a panel solid surface can be fixed due to two different mechanisms, adsorption or condensation. Especially in the case of adsorption, interaction between gas molecules and the foreign molecules of the substrate takes place and the interaction rate decreases with growing coverage. Because the adsorbent becomes saturated once a certain degree of surface coverage has been reached, only adsorbents of high adsorption capacity can be considered for practical applications. In the TITAN facility the sorption panel was coated with activated charcoal for pumping helium. For practical purposes, the ITER machine demands a certain pumping speed value to guarantee for a maximum allowable pressure (especially helium partial pressure) in the torus. However, to judge the underlying physics of the cryosorption process, it would be favourable to have a universal parameter which describes the interaction between the gas molecule and cold surface more neatly because pumping speed still depends on the molecular mass of the gas (see Eqs. 6.2 and 6.4). The sticking coefficient is such a feasible parameter. It decreases with rising temperature of the sorption panel and rising gas temperature; it decreases with increasing coverage and rising intake pressure.

For basic interpretations within the limits of our simplified model, the sticking coefficients can be estimated from the experimental results.

7 Evaluation of sticking coefficients

The sticking coefficients can be derived directly from the measured pumping speed, provided the transmission probability is known.

The measured pumping speed is determined according to the AVS Recommended Practice as [9]

$$S_{\text{meas}} = \frac{Q}{p - p_0} \quad (6.11)$$

where Q is the flow rate (throughput) and p_0 is the "ultimate" pressure prior to the experiment. Thus, the measured pumping speed refers to the inlet plane of the pump. Consequently, the capture probability as given by Eq. (6.3) must be related to the pump entrance (baffle) surface area A_{baffle} . Substituting A_{baffle} for A_{dome} into Eq. (6.3) gives

$$c(\alpha) = \frac{S_{\text{meas}}}{A_{\text{baffle}} \times \frac{V}{4}} \quad (6.12)$$

Further, the following relationship between the capture probability, the transmission probability and the sticking coefficient can be derived considering a system consisting of two components (the baffle and the pump) connected in series [10]

$$\frac{1}{c} = \frac{1}{w_{12}} + \frac{1}{\alpha} - 1 \quad (6.12a)$$

from which follows

$$\alpha = \frac{1}{\frac{1}{c} - \frac{1}{w_{12}} + 1} \quad (6.12b)$$

The transmission probability w_{12} of the shielded pump with the quilted panel contained in the TITAN structure was determined by the MOVAK3D calculations. It amounts to 0.1667. The smaller value of this combined transmission probability as compared with the calculated baffle transmission probability of $w_{\text{baffle}}=0.19$ is caused by the geometical arrangement of the quilted panel which is not orthogonal to the main flow direction.

In order to validate the theoretical value, additional experiments were performed. To evaluate the transmission probability pumping speed tests were made with nitrogen whose sticking coefficient at LHe-cooled charcoal is well known to be $\alpha_{\text{N}_2}=1.0$ [10]. In this case, according to Eq. (6.12a), the combined transmission probability w_{12} becomes equal to the capture probability and can be derived directly from the measured data (Eq. (6.12)).

Two measured pumping speed curves for nitrogen are depicted in Fig. 13. The first curve illustrates the pure molecular flow regime with constant values for pumping speed, whereas the second refers to the transition flow with increasing pumping speed. Judging from the low pressure pumping speed limit of about 3.5 m³/s (at reference temperature of 273.15 K) the value $w_{12}=0.141$, lying within the bounds of the maximum measurement uncertainty of about 20 % (calculated by the error propagation analysis), will finally be obtained for the transmission probability.

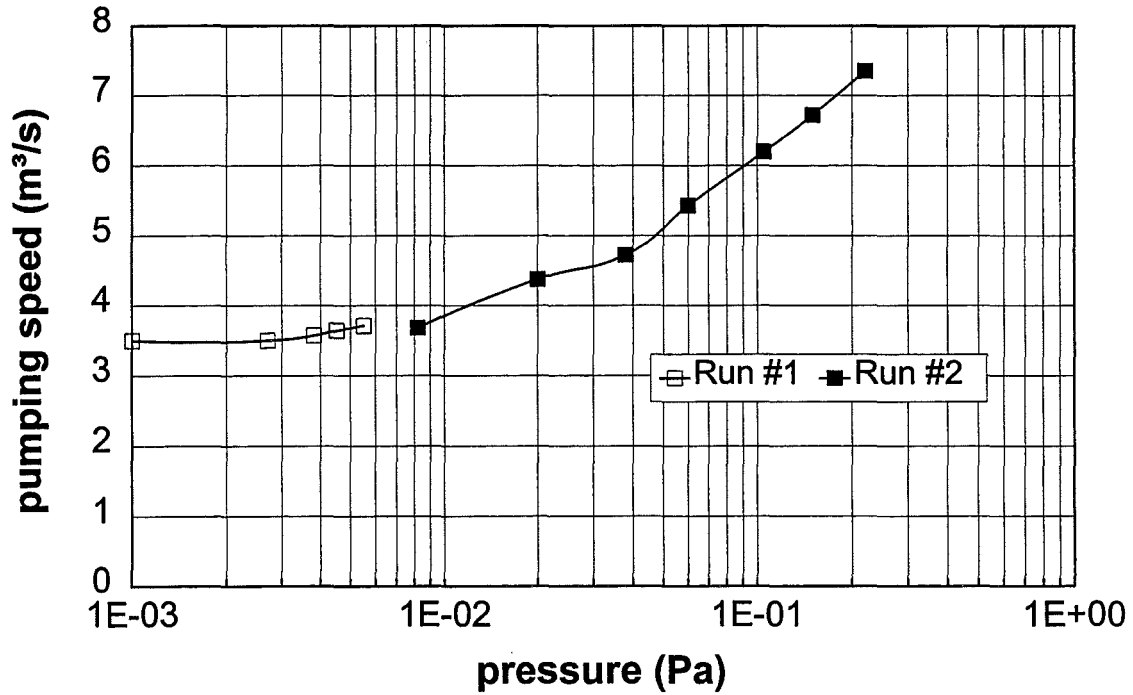


Figure 13. Measured pumping speeds for nitrogen with the panel in quilted geometry.

Thus, from Eq. (6.12b) results

$$\alpha = \frac{1}{\frac{1}{c} - 5.0} \quad (6.12c)$$

The capture probability for the shielded pump with the circular panel can be calculated using the formula [10]

$$c = \frac{1}{\frac{A_{\text{baffle}}}{A_{\text{panel}} \alpha} + \frac{1}{w_{\text{baffle}}} - 1} \quad (6.12d)$$

by substituting $\alpha=1$. In this case slightly lower capture probability w_{12}^c of 0.156 is obtained.

At the TITAN facility, an extensive test campaign - comprising both panel types - was performed to assess the pumping characteristics for ITER-relevant gases and gas

mixtures. As discussed above, the pumping of the pure hydrogens and inert gases at LHe-cooled activated charcoal is based on sticking coefficients which are very close to unity [10], except for helium which offers significantly smaller sticking coefficients.

The sticking coefficients of helium were evaluated for the panel in quilted geometry according to Eqs. (6.12) and (6.12b), using the recent experimental results. They are plotted in Fig. 14 as a function of the surface coverage relative to the maximum gas load. The sticking coefficients for the circular panel determined according to Eqs. (6.12) and (6.12d) are shown for comparison as well.

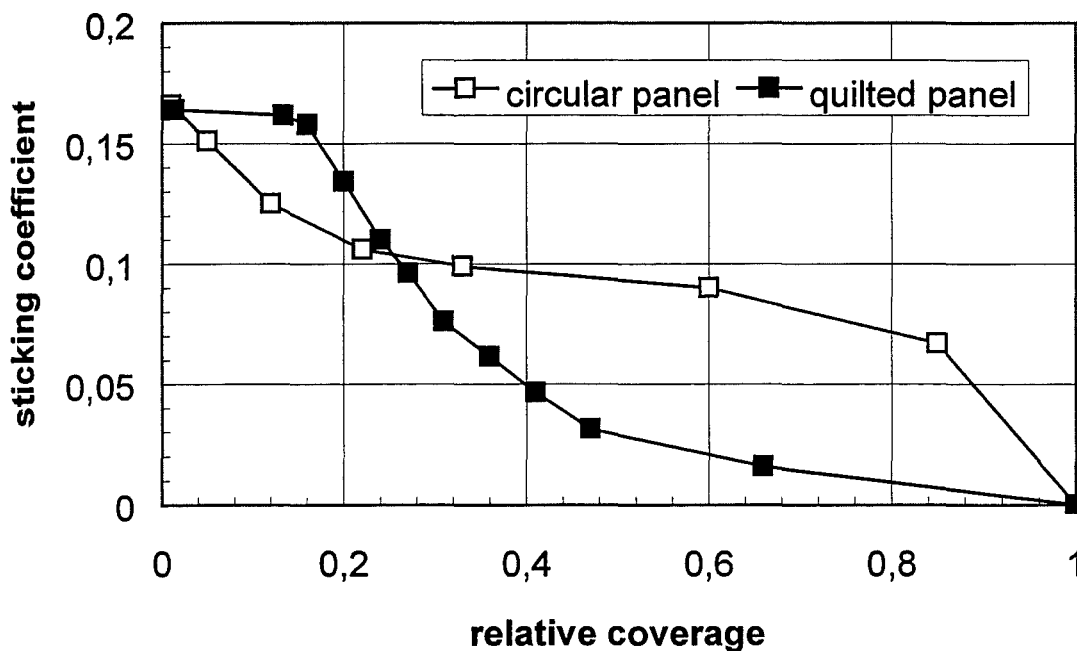


Figure 14. Helium sticking coefficients versus relative coverage obtained from the measured pumping speed.

7.1 Investigation for pure helium gas

The cryosorption pump has no constant pumping speed for helium, since, as already mentioned, the sticking coefficient α depends on the relative surface coverage (referenced to the maximum gas load). The value of α drops as the surface coverage increases, at first slowly (for a coverage lower than 0.2), then more rapidly, until it becomes zero at the maximum coverage value of 1 (cf. Fig. 14). In order to consider

this phenomenon in the MOVAK calculations, an option with variable sticking coefficients must be chosen while specifying the features of panel surfaces.

Within the MOVAK code, the behaviour of the sticking coefficient depending on the mean molecular coverage can be approximated by choosing a pre-defined shape function [6], whose parameters must be properly adjusted to fit the curve previously determined from the experimental data. Available shape functions cover a wide range of basic curves and include square root, linear, quadratic and partial linear functions. For the first three, only one additional input parameter must be provided. To determine a partial linear shape, four additional factors f_0, f_1, f_2, f_4 must be set up. Factor f_0 is identical to the highest sticking coefficient at the relative coverage of 0. For a relative coverage of 1, the sticking coefficient is always 0. Factor f_1 equals the value of relative coverage, at which the sticking coefficient is $f_0 \times f_2$. Moreover, a very practical S-shaped fit can be used, which is based on the polynomial representation

$$y(x)=f_0 (ax^n -bx^m) \quad (6.13)$$

with $m,n \in [1,20], f_0 \in [0,1]$.

and $y(x)=f_0$ for $x=0$

The application of the latter requires the definition of three parameters f_0, m and n . As before, f_0 is the highest possible value of the sticking coefficient for fresh regenerated panel. Constants a and b result from the boundary conditions.

A maximum molecular coverage on the absorbing surfaces is to be specified by the user. This figure represents the highest possible weight that may be deposited on all absorbing surfaces with variable sticking coefficients. In other words, when in course of the simulation the weight deposited on all surfaces with a variable sticking coefficient will attain this value, the saturation point (maximum coverage) will be reached and the relative coverage will be set to one. Balance tables in the MOVAK3D output list contain the percentage of the maximum molecular coverage achieved for all surfaces defined as absorbers with variable sticking coefficients. This additional information may be useful in the prediction of the saturation point of the adsorbent for a given geometrical configuration.

To gain an insight into the characteristics of the helium pumping process, a series of four MOVAK3D simulations was performed, employing variable sticking coefficients as given in Fig. 14. To approximate the functional dependence of Fig. 14, an S-shape function furnished with suitable parameters was chosen. A batch of 100 000 He gas molecules was emitted in each simulation run. The batch restart mode was activated.

This allowed to transfer the results of one Monte Carlo run to the subsequent simulations, hence, making the simulations dependent on each other. The simulation series began with the fresh, regenerated panel (relative coverage 0), the first batch scores were analysed and the results were recorded. In the following runs, the relative coverage was updated and the absorption rate was recalculated. The capture and the backscatter probability were estimated as well. The calculated capture probability vs. the relative molecular coverage of the panel is depicted in Fig. 15. It is clearly shown that the change of the capture probability when varying the sticking coefficient is less than proportional.

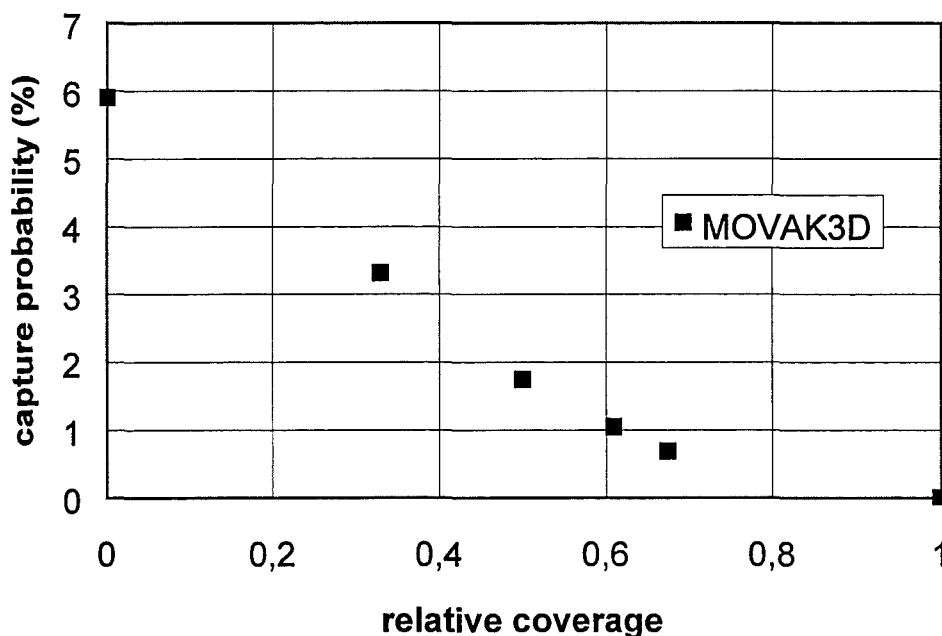


Figure 15. Helium pumping. Capture probability of the TITAN structure versus the relative molecular coverage.

7.2 Investigation for helium-containing mixtures

An experimental investigation on helium-containing gas mixtures was performed to gain more information about the influence of helium in a mixture. The ITER plasma exhaust gas is composed of one major component (H_2 , D_2 , DT , He , depending on the

operation mode) plus additional impurity fractions (CH_4 , CO_2 , CO , H_2O , O_2 etc.). Therefore, the systematic investigation was not made with pure H_2 or D_2 , but with so-called H_2 -base and D_2 -base mixtures, respectively; the base mixture consisted of 96.2 mol-% of H_2 or D_2 and 3.8% ITER-typical impurities. However, the tests revealed that the influence of the impurities is negligible in their low-content range. The detailed pumping speed results have been reported elsewhere [3, 12].

In Fig. 16, the derived sticking coefficient curves for pure helium and 4 pseudobinary mixture compositions measured with the quilted panel under LHe cooling conditions are given as a function of gas load. Gas load and pumping speed are referenced to a temperature of 273 K; the composition is indicated in mol-%. For ITER, the maximum He content is specified to be 10% [2]. It becomes obvious that the sticking coefficient of the pure hydrogens is drastically reduced when helium is present in the mixture. However, this deteriorating influence of helium is less critical for mixtures with deuterium than it is for protium. The figure also illustrates that in the composition range investigated the overall sticking coefficient of a protium/helium mixture may even become smaller than that of pure helium, whereas the helium curve and the deuterium/helium mixture curves do not intersect. Nevertheless, the saturation point (maximum coverage) is very much the same of about $0.6 \text{ (Pa}\cdot\text{m}^3\text{)/cm}^2$ for all mixtures investigated. It is shown that the resulting sticking coefficient curve for helium/hydrogen mixtures cannot be predicted by combining the pure gas properties according to their nominal composition ratio in the mixture.

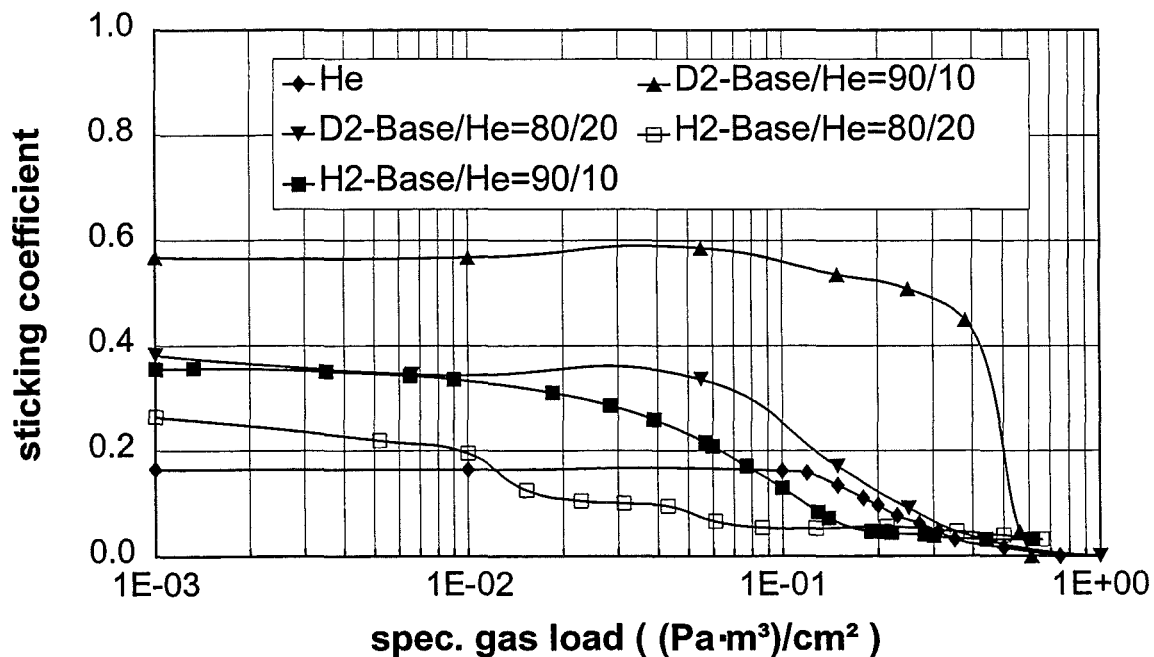


Figure 16. Sticking coefficient curves derived from experimental pumping speed tests with different gases. The nominal composition of the hydrogen/helium mixtures is indicated in mol-%.

This can be explained by the competitive sorption situation for the pumping of helium and hydrogen. As discussed in a previous paper [12], deuterium is partly condensed at the charcoal surface, whereas protium, and of course also helium, is almost only sorbed. Consequently, there is a strong competition for the active sorption sites at the charcoal surface, which is more intense for the combination protium and helium. The monitoring of the composition changes during pumping indicates that hydrogen is pumped to the disadvantage of helium. Consequently, this effect leads to a strong enrichment of helium [3, 13]. For the helium/deuterium mixtures, this does not affect the model calculation, as both species have practically the same mass number which is the only gas-typical parameter incorporated in the model. In the case of the H₂-base/helium system, a maximum He enrichment of 70% was found. If this real composition is considered in Eq. 6.12 for the derivation of the sticking coefficient, the capture probability is increased up to 10%, which leads to an increase in the sticking coefficient of about 20%. The sticking coefficient curves for both cases are compared in Fig. 17. However, the general conclusions drawn from Fig. 16 still remain valid.

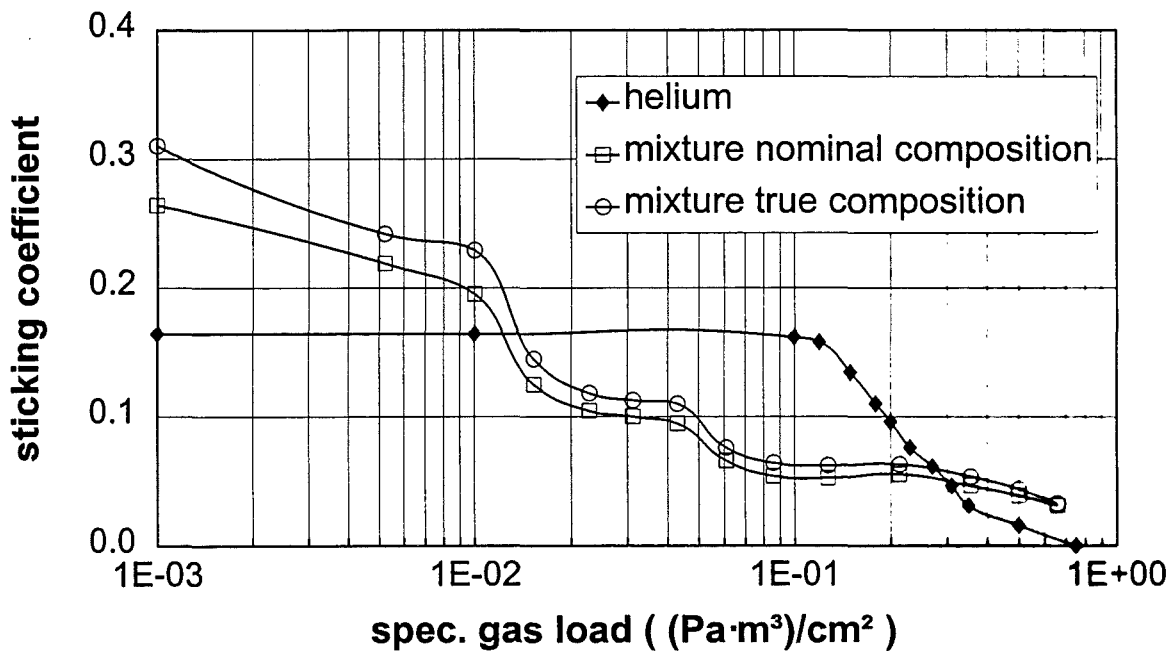


Figure 17. Illustration of the influence of composition changes during the pumping of gas mixture. Comparison for a mixture of a nominal composition of 20% He/80% H₂-base.

8 Application limits of the test-particle Monte Carlo method

The typical dependence of the measured pumping speed curves on the gas pressure at a variable flow rate is exemplified in Fig. 18 for deuterium tests at the LHe-cooled quilted panel [3]. The pumping speed decreases in the pressure range from 10^{-4} Pa until 6×10^{-3} Pa due to a limitation of diffusive mass transfer inside the charcoal pores and increases in the subsequent pressure interval up to 1.4×10^{-1} Pa. At pressures in the latter range, the mean free path becomes comparable with the entrance aperture dimension of the cryopump and, therefore, the flow regime is in transition from molecular to viscous. In this transition regime, the conductance to the pump is proportional to the pressure and leads to the conductance enhancement which may explain the results shown in Fig. 18.

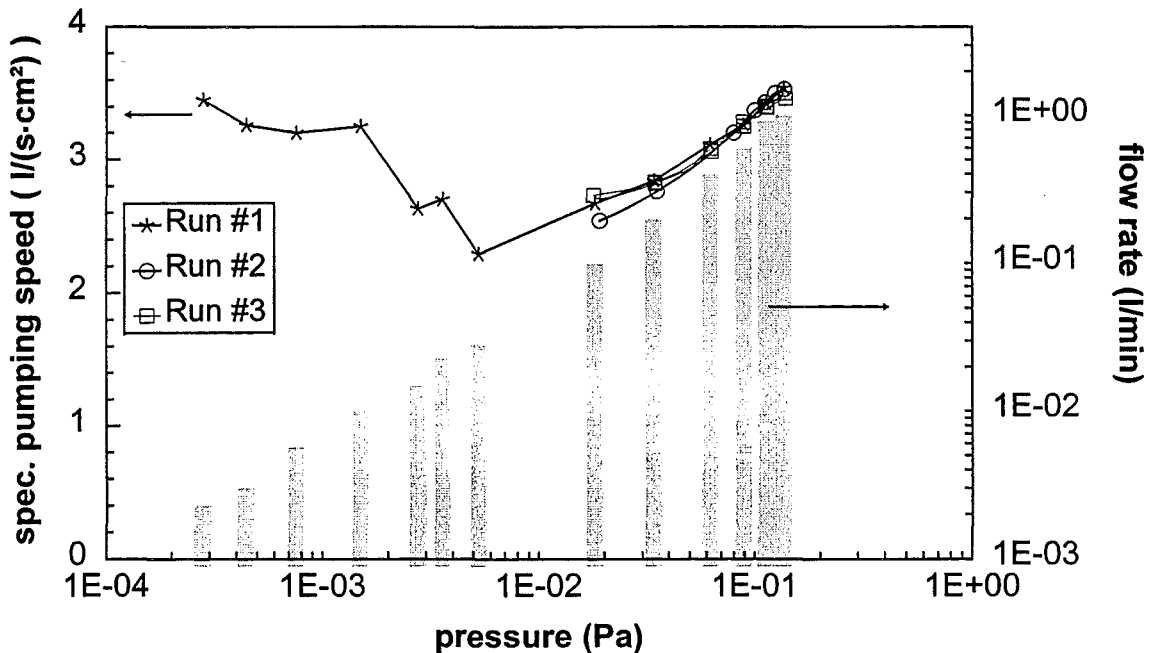


Figure 18. Experimental pumping speed results for pure D_2 and the LHe-cooled quilted panel as a function of pressure and adjusted flow rate.

The geometry of the pump and its surroundings is not easily amenable to a quantitative estimation of the effects of pressure on the conductance, but an approximate linear dependence of conductance on pressure is observed in simpler geometries such as an aperture.

In the transition regime, it becomes necessary to compute typical intermolecular collisions in addition to the molecule-surface interactions [7]. This can only be done, if there is already the representation of the complete flow field. The distribution

function must be chosen for this representation and, as in the finite difference method, it must be stored at the number of locations in phase space. The classical Monte Carlo method therefore shares a major disadvantage of the finite difference method: An initial estimate must be made with respect to the distribution function over the whole flow field. A large number of the test particle trajectories are to be computed with the assumed distribution serving as a target gas for the computation of typical intermolecular collisions. An updated target distribution is then constructed from the history of the test or incident molecules. The process is continued until there is no difference between the target and the incident distributions.

The alternative to the test-particle approach is to introduce a time variable and to follow the trajectories of a very large number of simulated molecules simultaneously in the computer. This method, called the direct-simulation Monte Carlo method, should be applied in the transition flow regime [7]. However, it requires the development of new calculation tools.

9 Remarks on the Monte Carlo precision

Monte Carlo results represent an average of the contributions by many histories sampled during the course of the problem. They are obtained by sampling possible random walks and assigning a score x_i to each random walk. Random walks typically will produce a range of scores depending on the calculated quantity and the variance reduction technique chosen. Thus, an important quantity is the statistical error or uncertainty associated with the result [14].

Suppose $f(x)$ is the history score probability density function for selecting a random walk that scores x to the quantity estimated. The true answer (or mean) is the expected value of x , $E(x)$, where

$$E(x) = \int xf(x)dx \quad \text{is a true mean value.} \quad (8.1)$$

The function $f(x)$ is seldom known explicitly; thus, the Monte Carlo random walk process implicitly samples $f(x)$. The true mean is then estimated by the sample mean

$$\bar{x} = \frac{1}{N} \sum_1^N x_i \quad (8.2)$$

where x_i is the value of x selected from $f(x)$ for the i^{th} history and N is the number of histories calculated in the problem. The Monte Carlo mean \bar{x} is the average value of the scores x_i for all the histories calculated in the problem. The relationship between

$E(x)$ and \bar{x} is given by the Strong Law of Large Numbers which states that if $E(x)$ is finite, \bar{x} tends to the limit $E(x)$ as N approaches infinity.

The variance of the population of x values is a measure of the spread in these values and given by

$$\sigma^2 = E(x^2) - (E(x))^2 \quad (8.3)$$

The square root of the variance is called the standard deviation of the population of scores. As with $E(x)$, σ is seldom known but can be estimated by Monte Carlo as S , given (for large N) by

$$S^2 = \overline{x^2} - \bar{x}^2 \quad (8.4)$$

and

$$\overline{x^2} = \frac{1}{N} \sum_{i=1}^N x_i^2 \quad (8.5)$$

The quantity S is the estimated standard deviation of the population of x based on the values of x_i that were actually sampled. The estimated variance of \bar{x} is given by

$$S_{\bar{x}}^2 = \frac{S^2}{N} \quad (8.6)$$

The estimated standard deviation of the mean \bar{x} is given by $S_{\bar{x}}$. It is important to note that $S_{\bar{x}}$ is proportional to $1/\sqrt{N}$, which is the inherent drawback of the Monte Carlo method. To halve $S_{\bar{x}}$, four times the original number of histories must be calculated. The quantity can also be reduced for a specified N by making S smaller, reducing the inherent spread of the results. This can be accomplished by using variance reduction techniques.

Error or uncertainty estimates for the results of Monte Carlo calculations refer to the precision of the result only and not to the accuracy. It is quite possible to calculate a highly precise result that is far from the physical truth because, nature has not been modelled correctly.

To define confidence intervals for the precision of a Monte Carlo result, the Central Limit Theorem of probability theory is used, stating that for large values of N and identically distributed random variables x_i with finite means and variances, the distribution of the resulting estimated means will be approximately normally distributed, with a true mean of $E(x)$. If S is approximately equal to σ , then

$$\bar{x} - S_x < E(x) < \bar{x} + S_x , \quad \sim 68\% \text{ of the time and} \quad (8.7)$$

$$\bar{x} - 2S_x < E(x) < \bar{x} + 2S_x , \quad \sim 95\% \text{ of the time} \quad (8.8)$$

from standard tables for the normal distribution function. Eq. (8.7) is a 68% confidence interval and Eq. (8.8) is a 95% confidence interval.

10 Conclusions

The pumping characteristics and performances of the TITAN test facility were extensively analysed in order to quantify the geometry impact on the measured pumping speed. For this purpose, the Monte Carlo Code MOVAK3D was employed. Three most important integral characteristics of the TITAN structure were estimated: The backscattering coefficient, the transmission and the capture probabilities. The method to calculate the sticking coefficients from the measured quantities was proposed on the basis of the analytical formula describing the dependence of the capture probability on the sticking coefficient and the transmission probability.

The most important results of the Monte Carlo analysis can be summarised as follows:

1. The transmission probability of the TITAN structure related to the cross-sectional area of the PNEUROP dome amounts to 0.1. The transmission probability of the pump and the baffle connected in series is 0.167. As a consequence, significant losses occur in the measured pumping speed as compared to the panel pumping speed.
2. The maximum capture probability (referenced to the PNEUROP dome) is equal to 0.0915 for the structure with the quilted panel. For the structure with the circular panel the maximum capture probability is 0.085. The capture probability related to the entrance area of the baffle reaches 0.167.
3. The contributions by two different quilted panel surfaces (front and rear) to the capture probability vary with the panel position due to a changing exposition to the main direction of the gas flow.
4. The pressure in the pump above the panel is reduced by one decade compared to the pressure in the PNEUROP dome.

5. The discrepancies which occurred between the measured specific pumping speed for the circular panel and the measured specific pumping speed for the quilted panel can be attributed to:
 - a relatively small increase of the measured pumping speed in the TITAN geometry with the quilted panel due to low conductance
 - a significant increase (factor 2.95) of the panel surface area.
6. The maximum helium sticking coefficients found for the quilted panel geometry and for the circular panel geometry are almost equal. However, the dependence of the helium sticking coefficient on the gas load is different for the two panel types investigated.
7. The relative decrease in the helium sticking coefficient with rising gas load does not fully affect the pumping speed, but is somewhat weakened.
8. The sticking coefficient of hydrogens is drastically reduced, if helium is added and may even become smaller than that of pure helium. The degree of deterioration is stronger for H_2 than for D_2 .

References

- [1] Day, Chr., Kammerer, B., Mack, A., Tests on Fast Heating for the Regeneration Process of ITER Cryopumps. Forschungszentrum Karlsruhe Report FZKA 5806, 1996.

- [2] Ladd, P., ITER EDA Design Description Document Vacuum Pumping System WBS 3.1, R 0.1. ITER Garching JWS, Nov. 1996.

- [3] Day, Chr., Kammerer, B., and Mack, A., Pumping Performance of Cryopanel Coated with Activated Carbon. Cryogenic Engineering Conference, Portland, USA, July 27-Aug. 1, 1997.

- [4] Class, G., 3D Monte Carlo-Simulation der Molekelbewegung und der Wärmestrahlung in Vakuum-Behältern-Rechenprogramm MOVAK3D-. Kernforschungszentrum Karlsruhe Report KfK 4292, 1987.

- [5] Saksaganskii, G., L., Molecular Flow in Complex Vacuum Systems. Gordon & Breach Science Publishers, 1988.

- [6] Class, G., Brockmüller, K., Hauer, V., Kernforschungszentrum Karlsruhe unveröffentlichter Bericht, 1987.

- [7] Bird, G., A., Molecular Gas Dynamics and the Direct Simulation of Gas Flows. Clarendon Press, Oxford, 1994.

- [8] Roth, A., Vacuum Technology. Elsevier Science Publishers B.V., Amsterdam, The Netherlands, 1990.

- [9] Hablanian, M., H., High-Vacuum Technology, second edition, revised and expanded. Marcel Dekker, New York, 1997.

- [10] Haefer, R., A., Cryopumping Theory and Practice. Clarendon Press, Oxford, 1989.

- [11] Day, Chr., Schwenk-Ferrero, A., Pumping Speed and Selectivity Phenomena for Cryopumping of ITER Relevant Exhaust Gas Mixtures. 17th IEEE/NPSS Symposium on Fusion Engineering, San Diego California, October 6-10, 1997.

- [12] Day, Chr. and Mack, A., Investigation into Pumping Characteristics of ITER Cryopumps. ISFNT-4, Tokyo, Japan, April 6-11, 1997.
- [13] Day, Chr., The Use of a High Resolution Gas Mass Spectrometer System for Selective Detection of Helium and Deuterium. 2nd Int. Workshop on Vacuum Science, Magdeburg, June 1997. Accepted for publication in Vacuum.
- [14] Briesmeister, J., F., Ed., MCNP – A General Monte Carlo N-Particle Transport Code, Version 4A. Los Alamos National Laboratory Report LA-12625, 1993.